GEND-INF--034

DE83 000810

GEND-INF-034

TESTING AND EXAMINATION OF TMI-2 ELECTRICAL COMPONENTS AND DISCRETE DEVICES

Florante T. Soberano
United Engineers and Constructors, Inc.

Published November 1982

Technically Edited and Published
on Behalf of the GEND Group
by
EG&G Idaho, Inc.
Idaho Falls, Idaho 83415

Prepared for the
U.S. Department of Energy
Three Mile Island Operations Office
Under DOE Contract No. DE-AC07-76ID01570

ABSTRACT

This report discusses the approach and results of the in situ test conducted on TMI-2 reactor building electrical components and discrete devices. Also included are the necessary presumptions and assumptions to correlate observed anomalies to the accident.

CONTENTS

FIGURES

TABLES

TESTING AND EXAMINATION OF TMI-2 ELECTRICAL COMPONENTS AND DISCRETE DEVICES

INTRODUCTION

The proper operation of many electrical components and discrete devices was vital to the immediate TMI-2 accident recovery and will be to the long-term recovery. Yet many of these components and devices were not designed or qualified for this purpose. Examples are the reactor coolant pump motors that were operated to help stabilize plant conditions during the accident. In order to provide permissives for the pump startup, the corresponding oil lift and backstop lube oil pumps must be in operation and discrete devices such as oil pressure, flow, and reservoir level switches and cooling water flow switches must also function properly. These electrical components and discrete devices are non-1E and non-LOCA qualified.

Examples of Class 1E equipment that operated during the accident and continue to operate are the reactor building air-cooling fans and motor-operated and solenoid valves. The fans operate continuously to circulate air to cool the reactor building. The motor-operated and solenoid valves were operated a number of times during the accident recovery and reactor building isolation. Except for the four operating reactor building air-cooling fans and the reactor building purge valves, the condition of most of the electrical equipment and discrete devices in the reactor building is unknown.

TEST APPROACH

An objective of the Instrument and Electrical Equipment Survivability program is to determine survivability to the TMI-2 accident and the condition of the reactor building electrical components, placing emphasis on Class 1E and LOCA-qualified equipment. To achieve the objective, the ideal approach would be to retrieve the components from the reactor building and subject them to a detailed hands-on testing and examination. However, as a result of the accident a large quantity of fission products

was released to the reactor building, grossly contaminating equipment and causing high radiation levels. These conditions make removal of equipment and components prohibitive because of extremely high cost and equipment inaccessibility. Many pieces of equipment and devices of interest will not be accessible until the reactor core is removed and decontamination activities reduce radiation exposures to safe levels. The completion of these events is presently scheduled for 1985. During the interim, the prolonged exposure to the reactor building environment could cause further damage to the equipment and result in the loss of valuable information. To obtain maximum data and information on the equipment and to alleviate the possible loss of information, an in situ test program was developed.

IN SITU TEST

An in situ test is conducted from outside the reactor building, and the measurements are normally made at the cabinet where the cable connected to the reactor building outer penetration box is terminated. This procedure can be changed for accessibility or if high radiation levels exist in the test area.

The test program was planned so that initial tests performed on equipment and devices selected would be followed by periodic testing. This will allow monitoring for degradation of the device as a function of time. Tests were also planned for specific devices and equipment before and after operations that would alter the devices' environmental operating conditions, such as decontamination.

Basically, the test consists of static and dynamic measurements. The static test includes measurements of resistance, capacitance, inductance, insulation resistance, and time domain reflectometry (TDR). The dynamic tests include inrush and steady state current measurements, signal spectral content analysis, and time response measurements. Static measurements are taken on the equipment both in its as is condition and after dynamic tests, if dynamic tests are performed.

CONDUCT OF TEST

Inductance and capacitance were measured using impedance (LCR) bridge Models HP-4261A or -4262A at all available frequencies. Insulation resistance was measured using a high resistance meter with a range of 5×10^5 to 2×10^{16} ohms.

TDR measurements were made using a Tektronix Model 1502, set to the propagation velocity of air when the properties of the cable under test were not known. Otherwise the true propagation velocity constant was set on the test instrument. If a suspected fault or anomaly was observed, additional measurements were made at a higher resolution.

Dynamic measurements and analyses were performed using a digital signal analyzer and associated sensing devices. When the electrical noise signal was below 10 V ac, data recordings were made using a Honeywell 101 magnetic tape recorder.

One special test was the dynamic test on the Axial Power Shaping Rods (APSR). This test attempted to drive the APSRs into their fully inserted position using an auxiliary power supply. Acoustic detectors were installed on the motor tube of the APSR mechanisms to monitor the mechanical noise generated during rod insertion. This test complemented other tests conducted to estimate the degree of reactor core damage, and also established that the APSRs were in a satisfactory position for uncoupling.

Testing Problems

Several difficulties were associated with the in situ testing. The most predominant was the presence of high electrical noise on the circuit under test. The noise levels varied from a low of a few millivolts to a high of 70 V. In several instances, the noise interference with the test instruments was high enough to preclude obtaining meaningful data.

Two other major problems were associated with in situ testing. First was the inability to dynamically operate or actuate some devices. Without actuation, only the components or parts of the device electrically connected to the building outer penetration terminal box can be observed. The second major problem was the use of common wires inside the reactor building on parallel connected ciruits. Unless the common wires associated with the branch circuits are isolated, resultant data from the circuit under test become obscured by branch circuit effect thereby making the data interpretation very difficult.

TEST RESULTS ANALYSIS

The pre-gross-decontamination in situ testing revealed some very interesting results. They are summarized in Table 1. A description of the components and devices, tests performed, and results are presented in the following paragraphs.

Pre-Gross-Decontamination Experiment In Situ Test Results

The first series of in situ tests was conducted in October 1981 before the commencement of the reactor building gross-decontamination experiment. Fifty-one pieces of equipment and devices were tested during the initial testing. This group was composed of 5 motor-operated valves, 6 motors, 4 solenoid valves, 11 CRDM stators, 11 CRD position indicators, and 14 on-off switches. Table 2 lists the 51 devices with their corresponding locations.

Level Switches

AH-LS-5006, -5007, and -5008 are three identical GEMS LS-1950 level switches. The switches are used for leak detection of the reactor building air-cooler coils. They furnish a signal for control room annunciation when a high level exists on the associated cooler condensate collection tray. The circuit has a 125-V dc potential. Figure 1 shows the interconnection wiring diagram of the three level switches.

TABLE 1. SUMMARY OF PRE-GROSS-DECONTAMINATION IN SITU TEST RESULTS

Device Identification	Test Point	Inductance	Capacitance	dc Resistance (ohms)	TDR Trace Number	Inrush/Holding Current (amps)	Insulation Resistance		Results
							Wire	ohms	
AH-LS-5006	CRAP-CRB2A	126.4 mH	--	554	3	NA	CRAP CRB2A	9.1×10^7 9.0×10^7	Very high contact resistance.
AH-LS-5007	CRAP-CRB3A	84 μH	--	1.30	4	NA	CRAP CRB3A	9×10^7 10×10^7	Device appears good.
AH-LS-5008	CRAP-CRB4A	81 μH	--	1.81	5	NA	CRAP CRB4A	7.6×10^7 7.6×10^7	Device appears good.
AH-EP-5037	64-N	--	--	--	--	0.5/0.2	64	3.8×10^8	Device is operational.
AH-EP-5040	74-N	--	--	--	--	0.6/0.2	74	3.7×10^8	Device is operational.
AH-KS-5037	65-66	--	--	3.9×10^8	--	NA	66	4×10^8	Device is operational.
AH-KS-5040	75-76	--	--	3.7×10^8	--	NA	76	5.7×10^8	No response. Setting might be incorrect.
AH-V6	14-N 15-H 16-H	-- -- --	-- -- --	4.75×10^5 1.28 3.55	10 10 10	0.5/0.5 NA --	-- NA --	-- NA --	"OPEN" limit switch is stuck closed. Solenoid operated within design limit.
AH-V74	64-2N	--	--	--	--	1.1/1.1	--	--	Solenoid operated within design limits.
NM-PS-4174 NM-PS-4175	CAP-CD3A --	NA --	NA --	2.05 --	14 --	NA --	CD3A CRAP	3.4×10^7 3.4×10^7	Contact of NM-PS-4174 is fused closed or instrument is out of calibration. NM-PS-4175 is in normal state.
RC56-PS1	2967A-2967B	132 μH	--	5.02	16	NA	2967A 2967B	6.9×10^6 7.8×10^6	Device is in normal state. In-containment cable has an impedance mismatch at midpoint.
RC58-FS1	2959A-2959B	--	11.24 μF	8.9×10^6	17	NA	2959A 2959B	8.6×10^6 2.5×10^6	Device is in the "actuated" state with no external influence. In-containment cable has an impedance mismatch at midpoint.
RC59-FS1	2975A-2975B	139 μH	--	5.17	18	NA	2975A 2975B	1.5×10^6 1.5×10^6	Device is in normal state. In-containment cable has an impedance mismatch at midpoint.

TABLE 1. (continued)

Device Identification	Test Point	Inductance	Capacitance	dc Resistance (ohms)	TDR Trace Number	Inrush/Holding Current (amps)	Insulation Resistance Wire	Insulation Resistance ohms	Results
RC60-LS1	2979A-2979B	137 μH	--	5.10	19	NA	2979A 2979B	1.3×10^6 1.3×10^6	Device is in alarm state. In-containment cable has an impedance mismatch at midpoint.
RC60-LS2	2982A-2982B	137 μH	--	5.16	20	NA	2982A 2982B	3.0×10^6 5.2×10^6	Device is in alarm state. In-containment cable has an impedance mismatch at midpoint.
RC67-VS1	A3VSP-A3VS	120 μH	--	Short	--	NA	A3VSP A3VS	-- --	Reset coil circuit is open.
	A3TVR-A3VSN	--	9.8 nF	9.8×10^7	--	Circuit open	A3TVR A3VSN	4.7×10^8 --	
RC67-VS3	B3VSP-B3VS	--	--	1.45×10^6	--	NA	--	--	Device is operational.
	B3TVR-B3VSN	--	--	1.15×10^3	--	133/132	--	--	
RC67-VS4	A4VSP-A4VS	--	25.5 nF	Open	--	NA	A4VSP A4VS	5×10^7 2.2×10^9	Device is operational.
	A4TVR-A4VSN	6.6 H	8.5 nF	1.044×10^3	--	180/180	A4TVR A4VSN	5.0×10^7 6.0×10^7	
RC-P-1A	T1-T2	6.55 mH	--	21	27	NA	T1	2.4×10^6	Abnormally high circuit dc resistance on motor windings, CTs and PTs. Unacceptably low insulation resistance of motor winding circuits Wire A3CM1 is evidently open.
	T1-T3	6.52 mH	--	21	27	NA	T2	2.5×10^6	
	T2-T3	6.52 mH	--	21	27	NA	T2	2.4×10^6	
	A3CM0-A3CM1	--	48.5 nF	Open	28	NA	--	--	
	A3CM0-A3CM2	--	--	336	28	NA	--	--	
	A3CM0-A3CM3	--	48 nF	325	28	NA	--	--	
	A3CM1-A3CM2	--		Open	--	NA	--	--	
	A3CM1-A3CM3	--	48 nF	Open	--	NA	--	--	
	A3CM2-A3CM3	--	--	145	--	NA	--	--	
	A3GC1-A3GC2	--	--	104	30	NA	--	--	
	A3RC1-A3RC2	--	--	216	29	NA	--	--	
	A3GP1-A3GP2	--	--	122	30	NA	--	--	
	A3RP1-A3RP2	--	--	195	29	NA	--	--	
RC-P-2B	T1-T2	6.5 mH	--	38	31	NA	T1	10^7	Abnormally high circuit dc resistance on motor windings, CTs and PTs.
	T1-T3	6.5 mH	78 nF at 10 kHz	38	31	NA	T2	10^7	
	T2-T3	6.5 mH	--	38	31	NA	T3	10^7	
	B3CM0-B3CM1	1100 μH at 10 kHz	--	100	32	NA	--	--	Marginal motor winding. Insulation resistance.
	B3CM0-B3CM2	1000 μH at 10 kHz	--	100	32	NA	--	--	

TABLE 1. (continued)

Device Identification	Test Point	Inductance	Capacitance	dc Resistance (ohms)	IDR Trace Number	Inrush/Holding Current (amps)	Insulation Resistance Wire	Insulation Resistance ohms	Results
RC-P-2B (continued)									
	B3CM0-B3CM3	880 μH at 10 kHz	--	104	32	NA	--	--	
	B3CM1-B3CM2	--	--	109	--	NA	--	--	
	B3CM1-B3CM3	--	--	105	--	NA	--	--	
	B3CM2-B3CM3	1700 μH at 10 kHz	--	103	--	NA	--	--	
	B3RC1-B3RC2	--	--	701	33	NA	--	--	
	B3RP1-B3RP2	--	--	685	34	NA	--	--	
	B3GC1-B3GC2	--	--	108	33	NA	--	--	
	B3GP1-B3GP2	--	--	88	34	NA	--	--	
RC-P-1A backstop lube oil pump Motor 2-1A-1	T1-T2	330 mH at 120 Hz	3.79 nF at 10 kHz	10.87×10^{3} [a]	36	NA	T1	5.1×10^{10}	The motor appears to be good. Insulation is good but may be dirty.
	T1-T3	320 mH at 120 Hz	3.78 nF at 10 kHz	10.46×10^{3} [a]	36	NA	T2	5.3×10^{10}	
	T2-T3	312 mH at 120 Hz	3.81 nF at 10 kHz	10.44×10^{3} [a]	36	NA	T3	5.4×10^{10}	
RC-P-1B backstop lube oil pump Motor 2-1B-1	T1-T2	365 mH at 1 kHz	4.16 nF at 10 kHz	81.8 [b]	37	NA	T1	3.4×10^{10}	The motor appears to be good. Insulation is good but may be dirty.
	T1-T3	338 mH at 1 kHz	4.08 nF at 10 kHz	77.8 [b]	37	NA	T2	3.4×10^{10}	
	T2-T3	357 mH at 1 kHz	4.14 nF at 10 kHz	81.3 [b]	37	NA	T3	3.4×10^{10}	
RC-P-1A backup oil lift pump	A1-A2	--	26.8 nF at 120 Hz	3.86×10^{6}	40	NA	A1 A2	6.8×10^{11} Open	A very high resistance at the armature. An open circuit exists on the field winding.
	F1-F2	--	5.2 nF at 120 Hz	Open	40	NA	Fa	3.1×10^{14} 3.9×10^{15}	
RC-P-2B backup oil lift pump motor	A1-A2	5.51 mH at 120 Hz	--	475	41	NA	A1 A2	5.2×10^{11} 5.2×10^{11}	The motor appears intact except for the high armature resistance.
	F1-F2	9.92 mH at 120 Hz	--	230	41	NA	F2	7.5×10^{11}	
CA-V1	T1-T2	205 mH at 120 Hz	3.13 nF at 10 kHz	37.7	--	--	T1	3.0×10^{6}	Motor appears to be normal except for marginal insulation resistance.
	T1-T3	205 mH at 120 Hz	3.17 nF at 10 kHz	37.7	--	--	T2	3.0×10^{6}	
	T2-T3	205 mH at 120 Hz	3.17 nF at 10 kHz	37.7	--	--	T3	3.0×10^{6}	
	1-60	--	--	--	--	NA	1 60	2×10^{5} 2.1×10^{5}	

TABLE 1. (continued)

Device Identification	Test Point	Inductance	Capacitance	dc Resistance (ohms)	TDR Trace Number	Inrush/Holding Current (amps)	Insulation Resistance Wire	Insulation Resistance ohms	Results
CA-V1 (continued)									
	1-70	--	14.05 nF at 1 kHz	--	--	NA	70	>2.0 x 10^8	
	1-45	81 mH at 1 kHz	--	--	--	NA	45	2.1 x 10^5	
	1-55	--	14.3 nF at 1 kHz	--	--	NA	55	>2.0 x 10^8	
CF-V1A	T1-T2	12.12 mH at 120 Hz	4.96[c]	--	--	--	T1	2.0 x 10^8	Motor winding appears to be good. Winding insulation appears good but may be dirty.
	T1-T3	12.21 mH at 120 Hz	4.96[c]	--	--	--	T2	2.0 x 10^8	
	T2-T3	12.50 mH at 120 Hz	4.96[c]	--	--	--	T3	2.0 x 10^8	
	1-55	--	3.22 x 10^7	--	--	NA	1 55	2.4 x 10^8 5.20 x 10^9	
	1-45	--	1.90	--	--	NA	45	1.21 x 10^9	
	GH-60	--	--	--	--	NA	GH 60	2.3 x 10^8 8 x 10^8	
RS-V100	GH-70	--	--	--	--	NA	70	7.8 x 10^8	Motor is good. An open circuit exist across wires 1 and 60.
	T1-T2	133.4 mH at 120 Hz	--	21.1	--	12.3 A/1.9A on T1	T1	9.17 x 10^9	
	T1-T3	134.8 mH at 120 Hz	--	21.1	--	13.8A/1.8A on T2	T2	6.48 x 10^{11}	
	T2-T3	118.1 mH at 120 Hz	--	21.1	--	11.1A/2.3A on T3	T3	6.1 x 10^{11}	
	1-60	--	--	Open	--	NA	1 60	1.2 x 10^8 2.6 x 10^8	
	1-70	--	--	Open	--	NA	70	2.6 x 10^8	
	1-45	--	--	0.01	--	NA	45	1.2 x 10^8	
	1-55	--	--	Open	--	NA	55	4.4 x 10^8	
RC-V1	T1-T2	58.6 mH at 120 Hz	--	8.58	--	--	T1	4.5 x 10^{11}	Motor appears to be good.
	T1-T3	60.3 mH at 120 Hz	--	8.59	--	--	T2	1.0 x 10^{11}	
	T2-T3	56.8 mH at 120 Hz	--	8.58	--	--	T3	1.4 x 10^{12}	
	1-60	--	--	1.9	--	NA	1 60	Infinity Infinity	
	1-70	--	--	--	--	NA	70 44	Infinity 1.0 x 10^8	

TABLE 1. (continued)

Device Identification	Test Point	Inductance	Capacitance	dc Resistance (ohms)	TDR Trace Number	Inrush/Holding Current (amps)	Insulation Resistance		Results
							Wire	ohms	
RC-V1 (continued)									
	44-45	--	--	2.03	--	NA	45	1.0×10^8	
	44-46	--	--	--	--	NA	46	1.0×10^8	
	55-56	--	--	--	--	NA	55	2.0×10^8	
							56	2.0×10^8	
	18A-18B	--	29 nF at 1 kHz	Open	--	NA	18A	2.0×10^8	
							18B	2.0×10^8	
	19A-19B	140 μH at 1 kHz	--	2.2	--	NA	19A	2.0×10^8	
							19B	2.0×10^8	
WDL-V271	T1-T2	439 mH at 1 kHz	--	101	--	--	T1	2.0×10^8	Motor appears to be good.
	T1-T3	442 mH at 1 kHz	--	100.8	--	--	T2	2.0×10^8	
	T2-T3	449 mH at 1 kHz	--	101	--	--	T3	2.0×10^8	
	1-60	75 μH at 10 Hz	--	1.17	--	NA	1	2.0×10^8	
							60	2.0×10^8	
	1-70	--	17.7 nF at 1 kHz	Open	--	NA	70	2.0×10^8	
	1-45	76 μH at 120 Hz	--	1.18	--	NA	45	2.0×10^8	
	1-55	--	25 nF at 1 kHz	Open	--	NA	55	2.0×10^8	
CRDM-ST01	A-N	222 mH at 120 Hz	--	7.89	--	NA	--	--	Stator appears to be good.
	B-N	223 mH at 120 Hz	--	7.87	--	NA	--	--	
	C-N	222 mH at 120 Hz	--	7.90	--	NA	--	--	
	AA-N	221 mH at 120 Hz	--	7.89	--	NA	--	--	
	BB-N	224 mH at 120 Hz	--	7.87	--	NA	--	--	
	CC-N	222 mH at 120 Hz	--	7.87	--	NA	--	--	
CRDM-ST35	A-N	213 mH at 120 Hz	--	7.91	--	NA	A-Grd.	1×10^{11}	Stator appears to be good.
	B-N	210 mH at 120 Hz	--	7.91	--	NA	--	--	
	C-N	210 mH at 120 Hz	--	7.90	--	NA	--	--	

TABLE 1. (continued)

Device Identification	Test Point	Inductance	Capacitance	dc Resistance (ohms)	TDR Trace Number	Inrush/Holding Current (amps)	Insulation Resistance		Results
							Wire	ohms	
CRDM-ST35 (continued)									
	AA-N	213 mH at 120 Hz	--	7.88	--	NA	--	--	
	BB-N	210 mH at 120 Hz	--	7.89	--	NA	--	--	
	CC-N	210 mH at 120 Hz	--	7.89	--	NA	--	--	
CRDM-ST50	A-N	214 mH at 120 Hz	--	7.97	--	NA	A-Grd.	1×10^{11}	Stator appears to be good.
	B-N	214 mH at 120 Hz	--	7.98	--	NA	--	--	
	C-N	214 mH at 120 Hz	--	7.96	--	NA	--	--	
	AA-N	213 mH at 120 Hz	--	7.95	--	NA	--	--	
	BB-N	217 mH at 120 Hz	--	7.96	--	NA	--	--	
	CC-N	214 mH at 120 Hz	--	7.97	--	NA	--	--	
CRDM-ST62	A-N	212 mH at 120 Hz	553 nF at 1 kHz	7.98	--	NA	A-Grd.	13×10^{9}	Stator appears to be good.
	B-N	210 mH at 120 Hz	59.7 nF at 1 kHz	7.96	--	NA	--	--	
	C-N	208 mH at 120 Hz	58.8 nF at 1 kHz	7.95	--	NA	--	--	
	AA-N	212 mH at 120 Hz	54.5 nF at 1 kHz	7.94	--	NA	--	--	
	BB-N	210 mH at 120 Hz	55.9 nF at 1 kHz	7.94	--	NA	--	--	
	CC-N	208 mH at 120 Hz	57.9 nF at 1 kHz	7.93	--	NA	--	--	
CRDM-ST63	A-N	222 mH at 120 Hz	139.1 nF at 10 kHz	8.05	--	NA	A-Grd.	4×10^{11}	Stator appears to be good.
	B-N	221 mH at 120 Hz	138.8 nF at 10 kHz	8.06	--	NA	--	--	
	C-N	219 mH at 120 Hz	139.2 nF at 10 kHz	8.06	--	NA	--	--	
	AA-N	222 mH at 120 Hz	136.7 nF at 10 kHz	8.08	--	NA	--	--	

TABLE 1. (continued)

Device Identification	Test Point	Inductance	Capacitance	dc Resistance (ohms)	TDR Trace Number	Inrush/Holding Current (amps)	Insulation Resistance Wire	Insulation Resistance ohms	Results
CRDM-ST63 (continued)									
	BB-N	221 mH at 120 Hz	137.5 nF at 10 kHz	8.08	--	NA	--	--	
	CC-N	220 mH at 120 Hz	137.8 nF at 10 kHz	8.09	--	NA	--	--	
CRDM-ST64	A-N	221 mH at 120 Hz	137 nF at 10 kHz	7.95	--	NA	A-Grd.	2×10^{12}	Stator appears to be good.
	B-N	218 mH at 120 Hz	137.2 nF at 10 kHz	7.97	--	NA	--	--	
	C-N	217 mH at 120 Hz	136.2 nF at 10 kHz	7.94	--	NA	--	--	
	AA-N	221 mH at 120 Hz	134 nF at 10 kHz	7.94	--	NA	--	--	
	BB-N	217 mH at 120 Hz	139 nF at 10 kHz	7.94	--	NA	--	--	
	CC-N	217 mH at 120 Hz	135.9 nF at 10 kHz	7.97	--	NA	--	--	
CRDM-ST65	A-N	221 mH at 120 Hz	137 nF at 10 kHz	7.91	--	NA	A-Grd.	10×10^{11}	Stator appears to be good.
	B-N	218 mH at 120 Hz	137.2 nF at 10 kHz	7.94	--	NA	--	--	
	C-N	217 mH at 120 Hz	136.2 nF at 10 kHz	7.90	--	NA	--	--	
	AA-N	221 mH at 120 Hz	134 nF at 10 kHz	7.91	--	NA	--	--	
	BB-N	218 mH at 120 Hz	139 nF at 10 kHz	7.92	--	NA	--	--	
	CC-N	217 mH at 120 Hz	139.5 nF at 10 kHz	7.96	--	NA	--	--	
CRDM-ST66	A-N	216 mH at 120 Hz	137.6 nF at 10 kHz	7.83	--	NA	A-Grd.	1.2×10^{9}	Stator appears to be good.
	B-N	214 mH at 120 Hz	136.5 nF at 10 kHz	7.85	--	NA	--	--	
	C-N	213 mH at 120 Hz	137.0 nF at 10 kHz	7.88	--	NA	--	--	
	AA-N	217 mH at 120 Hz	136.6 nF at 10 kHz	7.87	--	NA	--	--	
	BB-N	214 mH at 120 Hz	136.4 nF at 10 kHz	7.86	--	NA	--	--	
	CC-N	213 mH at 120 Hz	137.7 nF at 10 kHz	7.85	--	NA	--	--	

TABLE 1. (continued)

Device Identification	Test Point	Inductance	Capacitance	dc Resistance (ohms)	TDR Trace Number	Inrush/Holding Current (amps)	Insulation Resistance		Results
							Wire	ohms	
CRDM-ST67	A-N	209 mH at 120 Hz	134.3 nF at 10 kHz	7.93	--	NA	A-Grd.	6.8×10^{11}	Stator appears to be good.
	B-N	205 mH at 120 Hz	133.2 nF at 10 kHz	7.93	--	NA	--	--	
	C-N	203 mH at 120 Hz	135.8 nF at 10 kHz	7.94	--	NA	--	--	
	AA-N	207 mH at 120 Hz	131.8 nF at 10 kHz	7.95	--	NA	--	--	
	BB-N	205 mH at 120 Hz	134.8 nF at 10 kHz	7.95	--	NA	--	--	
	CC-N	203 mH at 120 Hz	134.0 nF at 10 kHz	7.93	--	NA	--	--	
CRDM-ST68	A-N	217 mH at 120 Hz	139.5 nF at 10 kHz	7.8	--	NA	A-Grd.	5.0×10^{9}	Stator appears to be good.
	B-N	218 mH at 120 Hz	138.8 nF at 10 kHz	7.8	--	NA	--	--	
	C-N	217 mH at 120 Hz	138.8 nF at 10 kHz	7.9	--	NA	--	--	
	AA-N	214 mH at 120 Hz	169.0 nF at 10 kHz	7.9	--	NA	--	--	
	BB-N	218 mH at 120 Hz	168.7 nF at 10 kHz	7.8	--	NA	--	--	
	CC-N	216 mH at 120 Hz	170.5 nF at 10 kHz	7.8	--	NA	--	--	
CRDM-ST69	A-N	229 mH at 120 Hz	169.0 nF at 10 kHz	8.0	--	NA	A-Grd.	5.2×10^{10}	Stator appears to be good.
	B-N	226 mH at 120 Hz	165.0 nF at 10 kHz	8.0	--	NA	--	--	
	C-N	225 mH at 120 Hz	167.6 nF at 10 kHz	8.0	--	NA	--	--	
	AA-N	229 mH at 120 Hz	166.0 nF at 10 kHz	8.0	--	NA	--	--	
	BB-N	225 mH at 120 Hz	167.5 nF at 10 kHz	8.0	--	NA	--	--	
	CC-N	225 mH at 120 Hz	166.5 nF at 10 kHz	8.0	--	NA	--	--	

a. Effective series resistance measured at 10 kHz.

b. Effective series resistance measured at 120 kHz.

c. Equivalent series resistance.

TABLE 2. LIST OF DEVICES TESTED

Device Tag	Type of Device	Elevation (ft)
AH-LS-5006	GEMS level switch	306
AH-LS-5007	GEMS level switch	306
AH-LS-5008	GEMS level switch	306
AH-EP-5037[a]	ASCO solenoid valve	342
AH-EP-5040[a]	ASCO solenoid valve	342
AH-KS-5037[a]	NAMCO limit switch	342
AH-KS-5040[a]	NAMCO limit switch	342
AH-V6[a]	Valcor solenoid valve	322
AH-V74[a]	Valcor solenoid valve	322
NM-PS-4174	SOR pressure switch	349
NM-PS-4175	SOR pressure switch	349
RC56-PS1	Barksdale pressure switch	322
RC58-FS1	M&M flow switch	322
RC59-FS1	M&M flow switch	322
RC60-LS1	SOR level switch	322
RC60-LS2	SOR level switch	322
RC67-VS2	Robertshaw vibration switch	322
RC-67-VS3	Robertshaw vibration switch	322
RC-67-VS4	Robertshaw vibration switch	322
RC-P-1A	Allis-Chalmers, 9000 hp, 6900 V ac induction motor	322
RC-P-2B	Allis-Chalmers, 9000 hp, 6900 V ac induction motor	322
RC pump backstop lube oil pump Motor 2-1A-1	1/2 hp, 480 V ac, 3-phase, induction motor	--

TABLE 2. (continued)

Device Tag	Type of Device	Elevation (ft)
RC pump backstop lube oil pump Motor 2-1B-1	1/2 hp, 480 V ac 3-phase, induction motor	322
RC-P-1A backup oil lift pump motor	10 hp, 230 V dc shunt-wound motor	322
RC-P-2B backup oil lift pump motor	10 hp, 230 V dc shunt-wound motor	322
CA-V1[a]	Motor operated valve	324
CF-V1A[a]	Motor operated valve	308
NS-V100[a]	Motor operated valve	319
RC-V1[a]	Motor operated valve	357
WDL-V271[a]	Motor operated valve	318
CRDM-ST01	CRD stator	345
CRDM-ST35	CRD stator	345
CRDM-ST50	CRD stator	345
CRDM-ST62	CRD stator	345
CRDM-ST63	CRD stator	345
CRDM-ST64	CRD stator	345
CRDM-ST65	CRD stator	345
CRDM-ST66	CRD stator	345
CRDM-ST67	CRD stator	345
CRDM-ST68	CRD stator	345
CRDM-ST69	CRD stator	345
CRDM-API-01	CRD position indicator	345
CRDM-API-35	CRD position indicator	345

TABLE 2. (continued)

Device Tag	Type of Device	Elevation (ft)
CRDM-API-50	CRD position indicator	345
CRDM-API-62	CRD position indicator	345
CRDM-API-63	CRD position indicator	345
CRDM-API-64	CRD position indicator	345
CRDM-API-65	CRD position indicator	345
CRDM-API-66	CRD position indicator	345
CRDM-API-67	CRD position indicator	345
CRDM-API-68	CRD position indicator	345
CRDM-API-69	CRD position indicator	345

a. Class 1E equipment.

The level switches are constructed of stainless steel with a magnet-equipped float that moves along the unit stem as collection tray levels change. A glass-enclosed, hermetically sealed reed switch installed within the unit's stem actuates when influenced by the magnet. Each switch is electrically connected to a NEMA 4 terminal box mounted on the side of the aircooler, as shown in Figure 2.

AH-LS-5007 and -5008 exhibited a circuit resistance of 1.30 and 1.81 ohms, respectively. These values are in close agreement with the calculated maximum circuit resistance of approximately 1.45 ohms. Likewise, the measured inductance for the devices of 84 and 81 μH compare well with the estimated value of 89 μH. The calculated values are based on an AWG 12 soft drawn copper conductor with a 3/64-in. thick insulation and a cable pulled length of 442 ft.

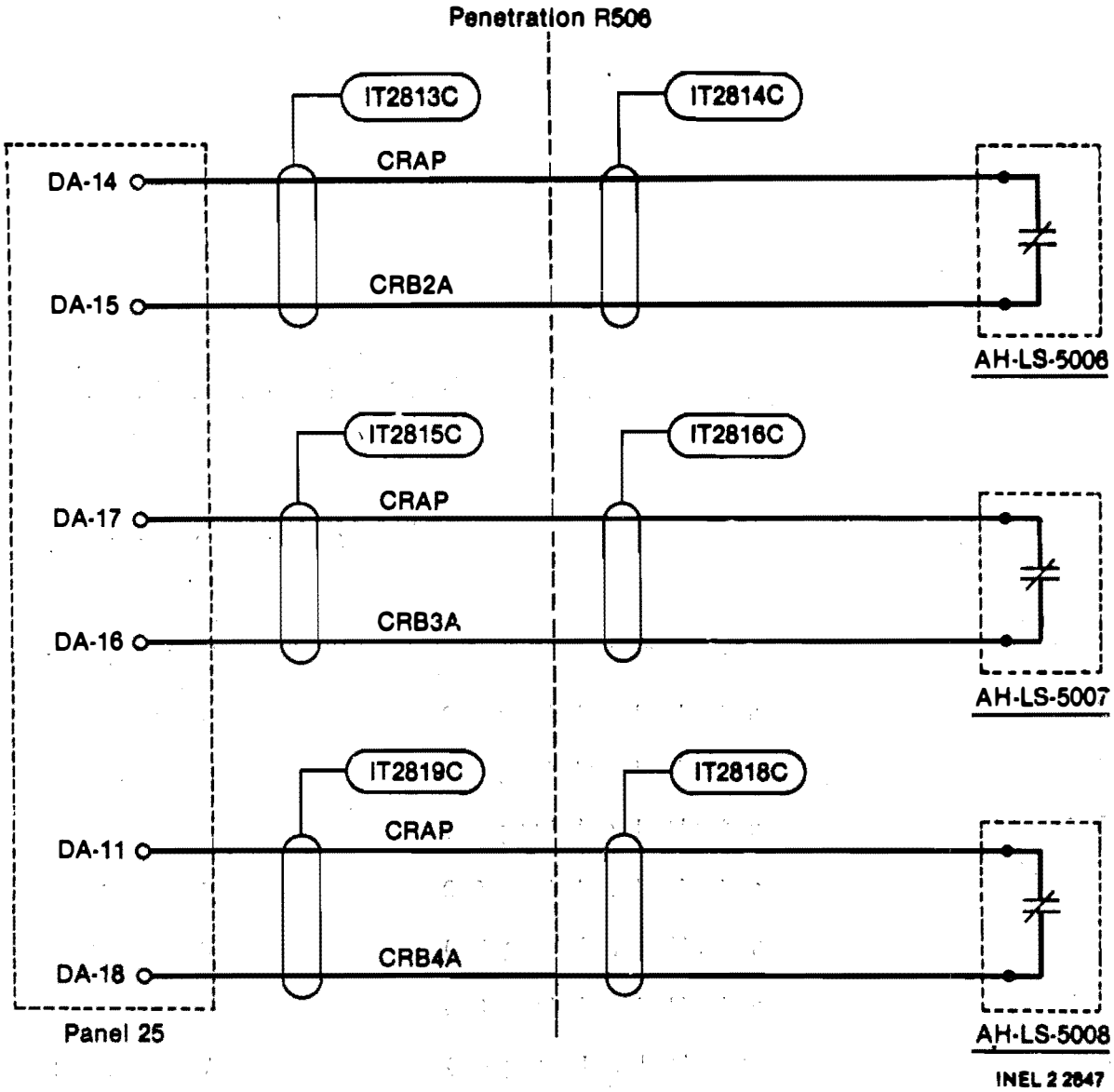

Figure 1. Interconnection wiring diagram of AH-LS-5006, -5007, and -5008.

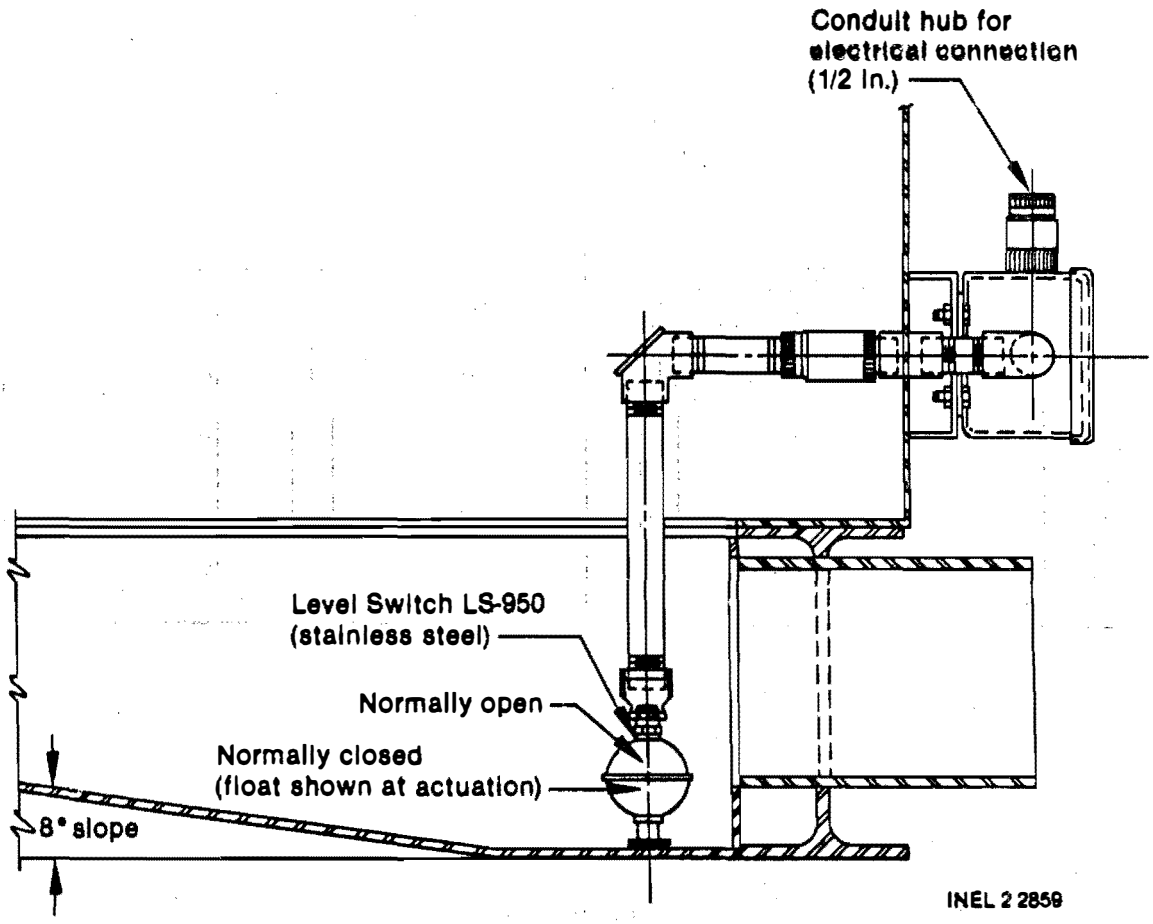

Figure 2. Mounting detail of AH-LS-5006, -5007, and -5008.

AH-LS-5006 exhibited an abnormally high circuit dc resistance of 554 ohms and inductance of 126.4 mH. The high resistance condition was confirmed by the TDR measurements shown in Figure 3 and is located at the equipment-end of the cable. The TDR trace also indicates a capacitive element at the termination, a condition which could be attributed to a wet or grossly corroded switch contact. The high resistance presented by AH-LS-5006, however, was not high enough to trip the associated annunciator circuit.

The TDR traces of AH-LS-5007 and -5008, shown in Figures 4 and 5 respectively, conform with the trace characteristic of a low resistance at cable termination. The measurements did not reveal any cable damage. The insulation resistance measurements on Circuits AH-LS-5006, -5007, and -5008 did not reveal any insulation breakdown.

Solenoid Valves

AH-EP-5037 and -5040 are ASCO Model HT8331A45 solenoid valves. These valves are actuating pilots for reactor building Purge Valves AH-V2B and -V3A, respectively. AH-KS-5037 and -5040 are NAMCO Severe Environment limit switches used for position indication of Purge Valves AH-V2B and -V3A. Two limit switches are provided on each purge valve. Both the solenoid valves and limit switches are designed to operate after being subjected to a maximum environmental condition of 286°F, 60 psig, 100% relative humidity and a total integrated dose of 2×10^7 rads. The devices have been extensively used for reactor building purging since the accident. Both solenoid valves and limit switches are Class 1E. Figure 6 shows the devices interconnection wiring diagram.

Solenoid Valves AH-EP-5037 and -5040 and their associated limit Switches AH-KS-5037 and -5040 were subjected to both static and dynamic tests. The insulation resistance of the circuits under test are all in the range of 3 to 5×10^8 ohms. Because the branch circuits were not isolated from the circuit under test, other static test data were obscured.

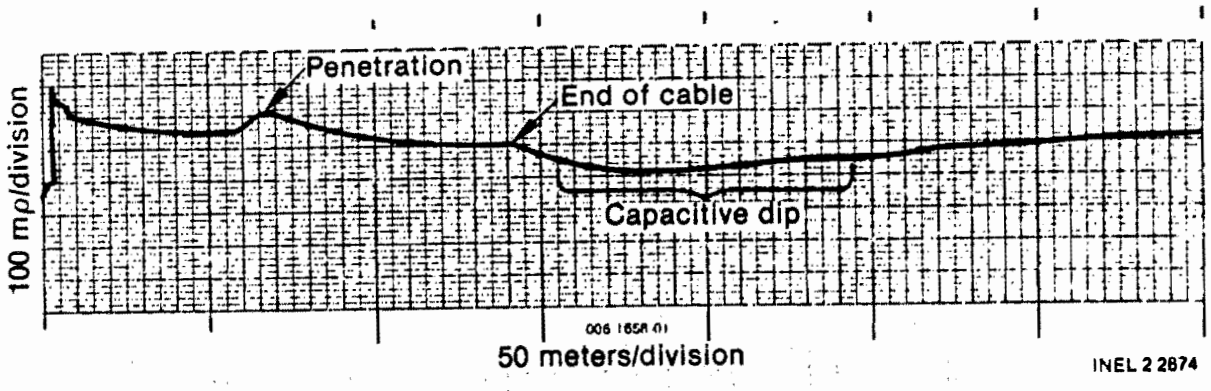

Figure 3. Pre-gross-decontamination TDR trace of AH-LS-5006.

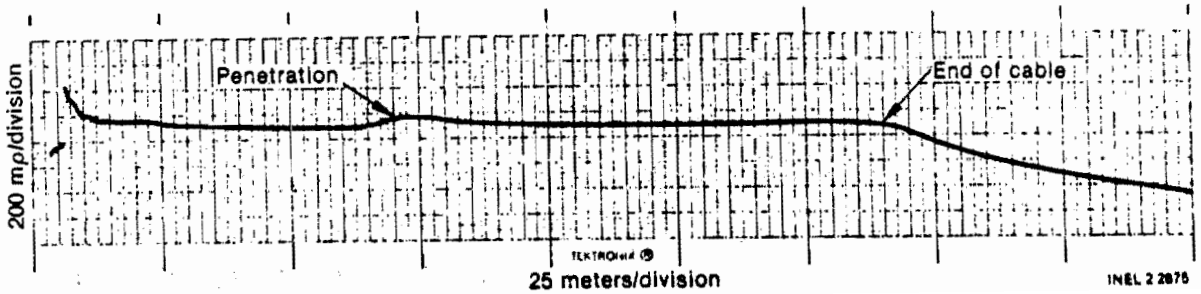

Figure 4. Pre-gross-decontamination TDR trace of AH-LS-5007.

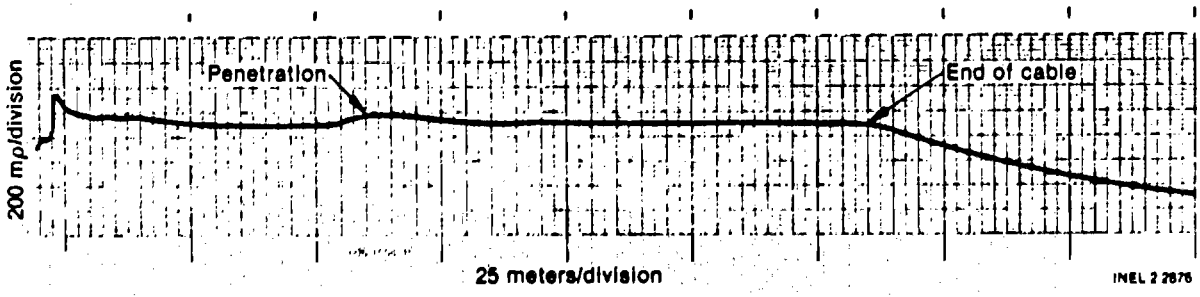

Figure 5. Pre-gross-decontamination TDR trace of AH-LS-5008.

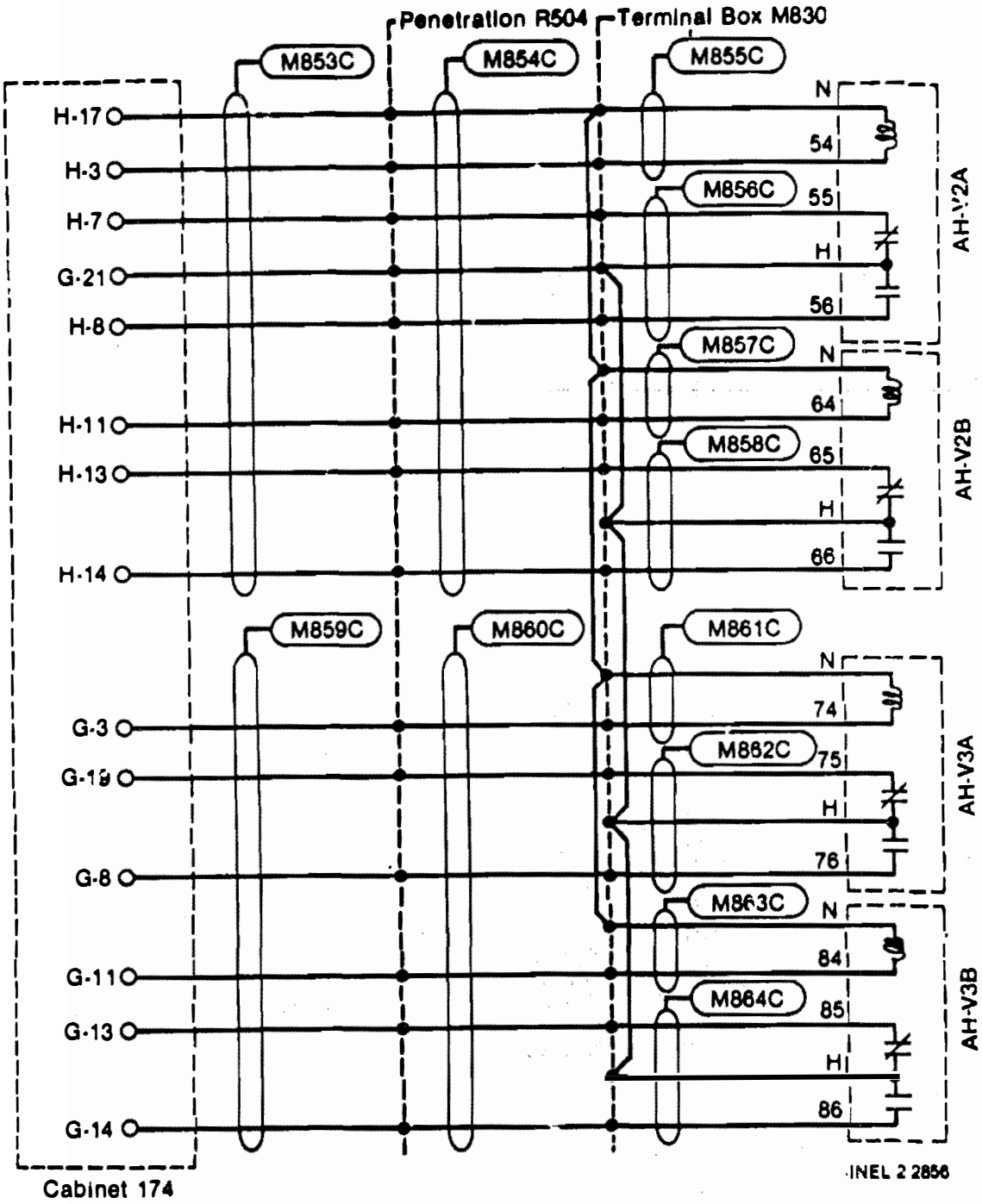

Figure 6. Interconnection wiring diagram of purge Valves AH-V2A, -V2B, and -V3B.

The dynamic test of the solenoid valves disclosed a holding current of about 0.2 amp. This value is within the design values of 0.225 amp based on 120 V ac, suggesting that the solenoid valves are operating normally. The dynamic test also revealed that the "OPEN" limit switch of AH-KS-5040 was not operating. The other limit switches (AH-KS-5037 and the "CLOSED" switch of AH-KS-5040) responded when their respective butterfly valves were operated.

AH-V74 and -V6 are VALCOR nuclear solenoid valves. Both valves are Class 1E equipment but were not LOCA qualified at the time of their manufacture. AH-V74, shown in Figure 7, is the pilot valve for the LOCA dampers in the reactor building. AH-V6 is a containment isolation valve in the reactor building pressure instrument line. Both valves are powered by a 120 V ac source and have an internal rectifier for the dc solenoid coil operation. A typical solenoid valve cross-section is shown in Figure 8. They are equipped with a NEMA 4 enclosure and a Class H coil. Each valve has two sets of SPST reed limit switches used for position indication. All the components of the solenoid valves are designed for environmental conditions of 286°F, 100% relative humidity, 53.2 psig, 7.5×10^6 rad/h, and total integrated dose of 2.8×10^7 rads. Figure 9 shows the solenoid valves' interconnection wiring diagrams.

AH-V74 was subjected only to a dynamic test. The attempt to perform the static test was cancelled due to high radiation and gross contamination in the test area. In the test, the inrush and holding currents were both measured at 1.1 amperes--less than the 1.5 amps maximum design.

AH-V6 was tested statically and dynamically. The static measurement was made with the valve closed. As expected, the CVC (closed when valve is closed) limit switch was closed and had a measured circuit resistance of 1.28 ohms--a value compatible with the cable pulled length of approximately 348 ft. It was also observed that the CVO (closed when valve is open) limit switch was closed and had a circuit resistance of 3.55 ohms. The dc resistance across the rectifier-coil circuit was much higher than expected. This discrepancy was later traced to the magnitude of the excitation signal of

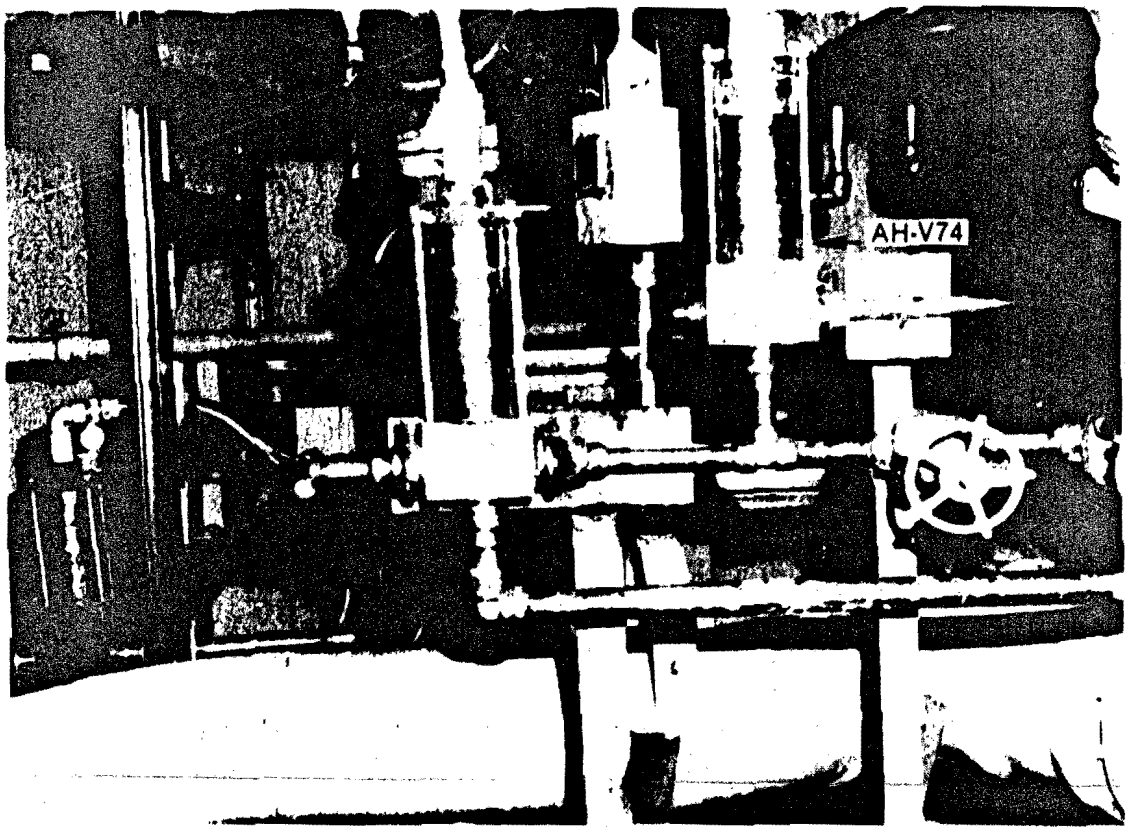

INEL 2 2596

Figure 7. Installation of AH-V74.

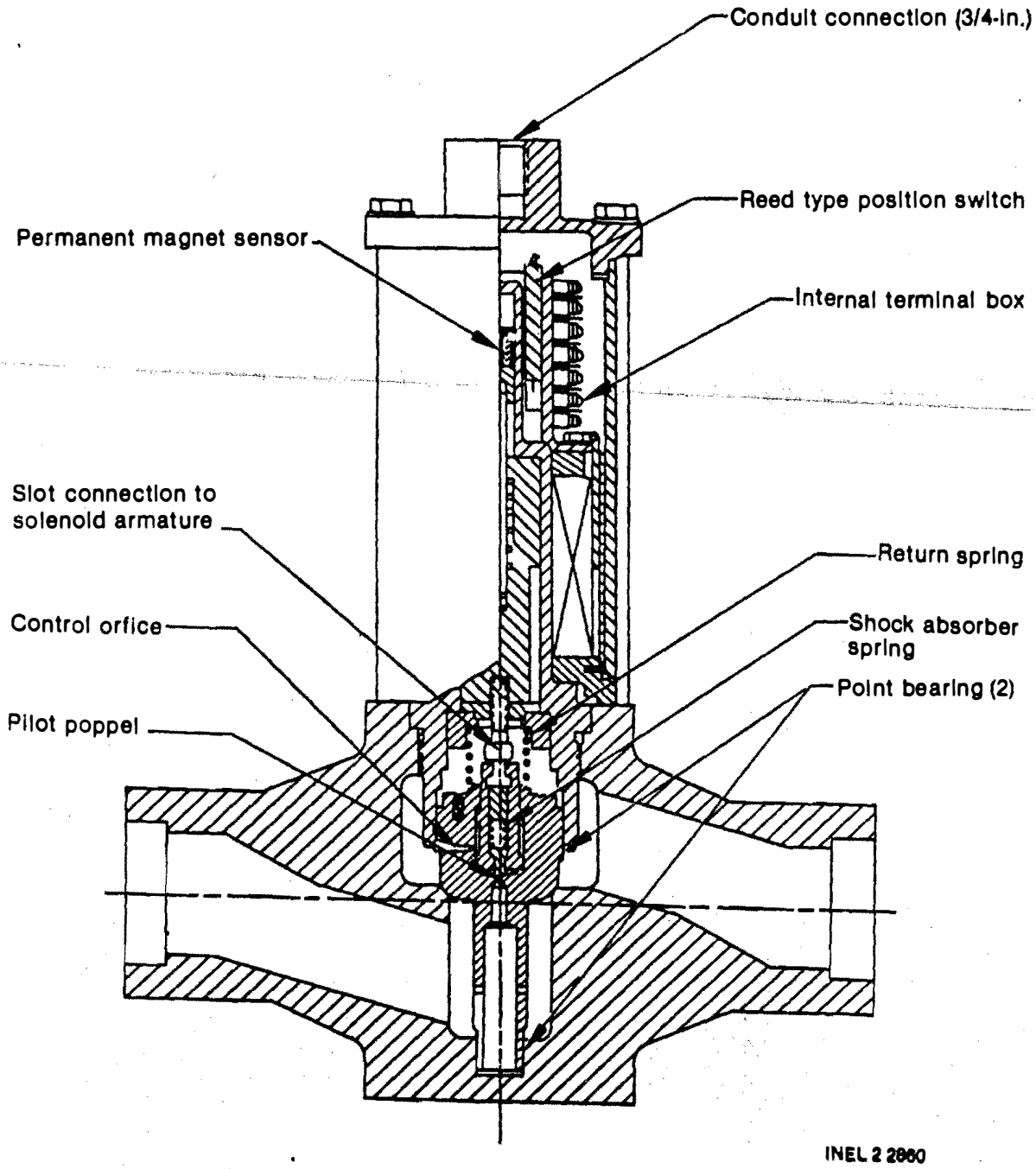

Figure 8. Cross-section of a typical VALCOR solenoid valve.

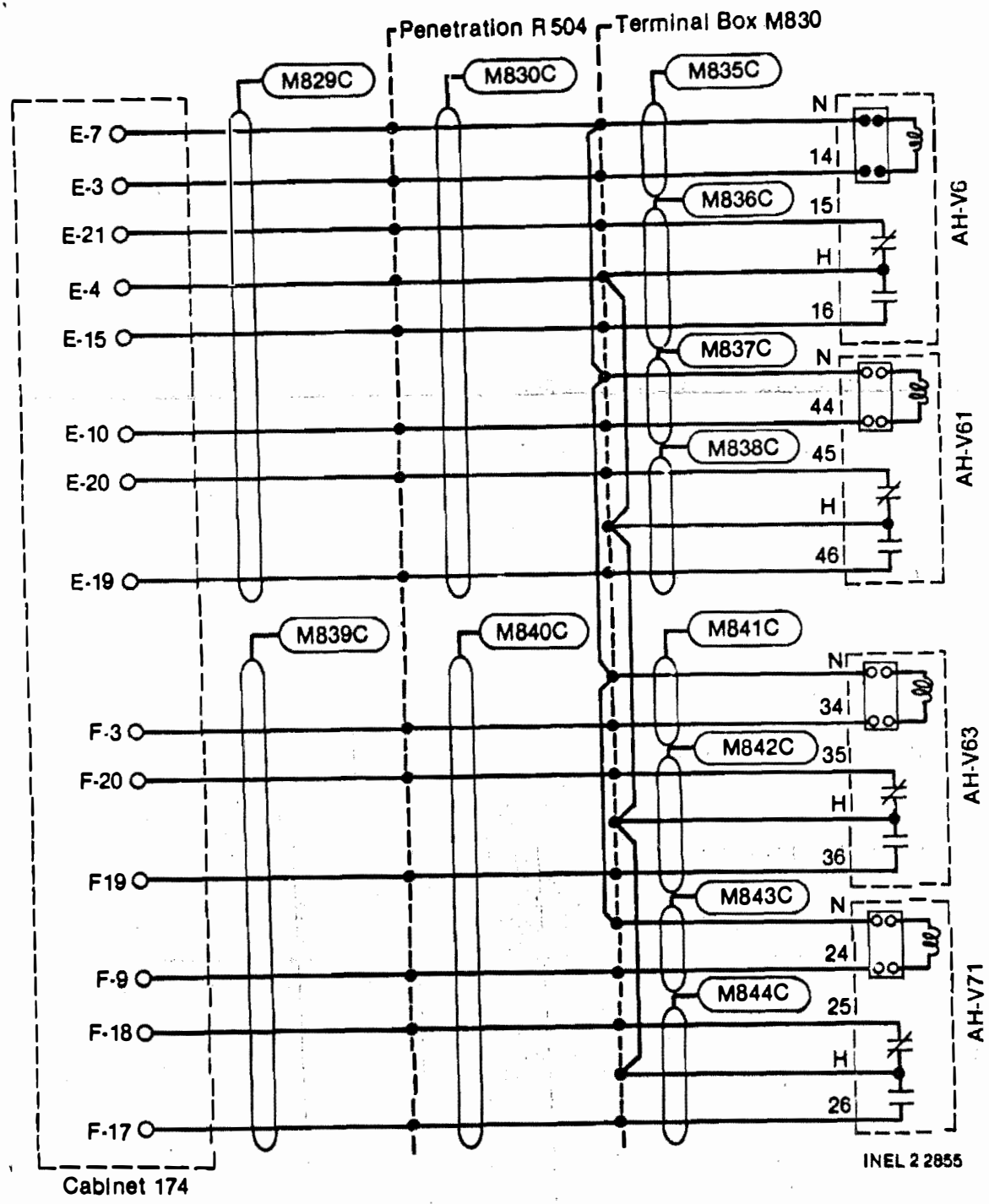

Figure 9. Interconnection wiring diagram of solenoid Valves AH-V6, -V61, -V63, and -V71.

the measuring instrument, which was insufficient to cause the rectifier diodes to conduct. The TDR traces shown in Figure 10 disclosed no cable fault.

The dynamic test on AH-V6 proved that the valve is operational. The measured inrush and holding currents were 0.5 amp--less than the maximum specified operating value of 1.5 amperes. It also confirmed the anomaly in the CVO limit switch. The switch, normally open when not under the influence of a magnetic field, did not respond when the valve was cycled. The CVC limit switch responded properly to the valve stem movement. Analysis of the CVO limit switch indicates that the contacts may have welded together.

Pressure Switches

Pressure Switches NM-PS-4174 and -4175 are used in the reactor building nitrogen system to monitor the nitrogen manifold pressure. They actuate an alarm when the manifold pressure is outside the operating range. They are mounted on Instrument Rack 432 as shown in Figure 11 and their interconnection wiring diagram is shown in Figure 12. Both pressure switches are force-balance piston-actuated assemblies made by Static-O-Ring. This type of switch is commonly used in other nuclear plants in, both 1E and non-1E class applications. A cutaway view of a typical unit is shown in Figure 13.

NM-PS-4174 and -4175 were statically tested in their "as is" state. Pressurization of the system to actuate the devices was not permitted due to the unknown condition of the remainder of the system. Both devices have indicated that their respective contacts are closed as determined by the dc resistance measurement and confirmed by the TDR trace shown in Figure 14. The circuit dc resistance of 2.05 ohms is in agreement with the expected maximum value of 2.33 ohms that corresponds to the cable pulled length. The TDR test also confirms the location of the low resistance point to be at the device-end of the cable.

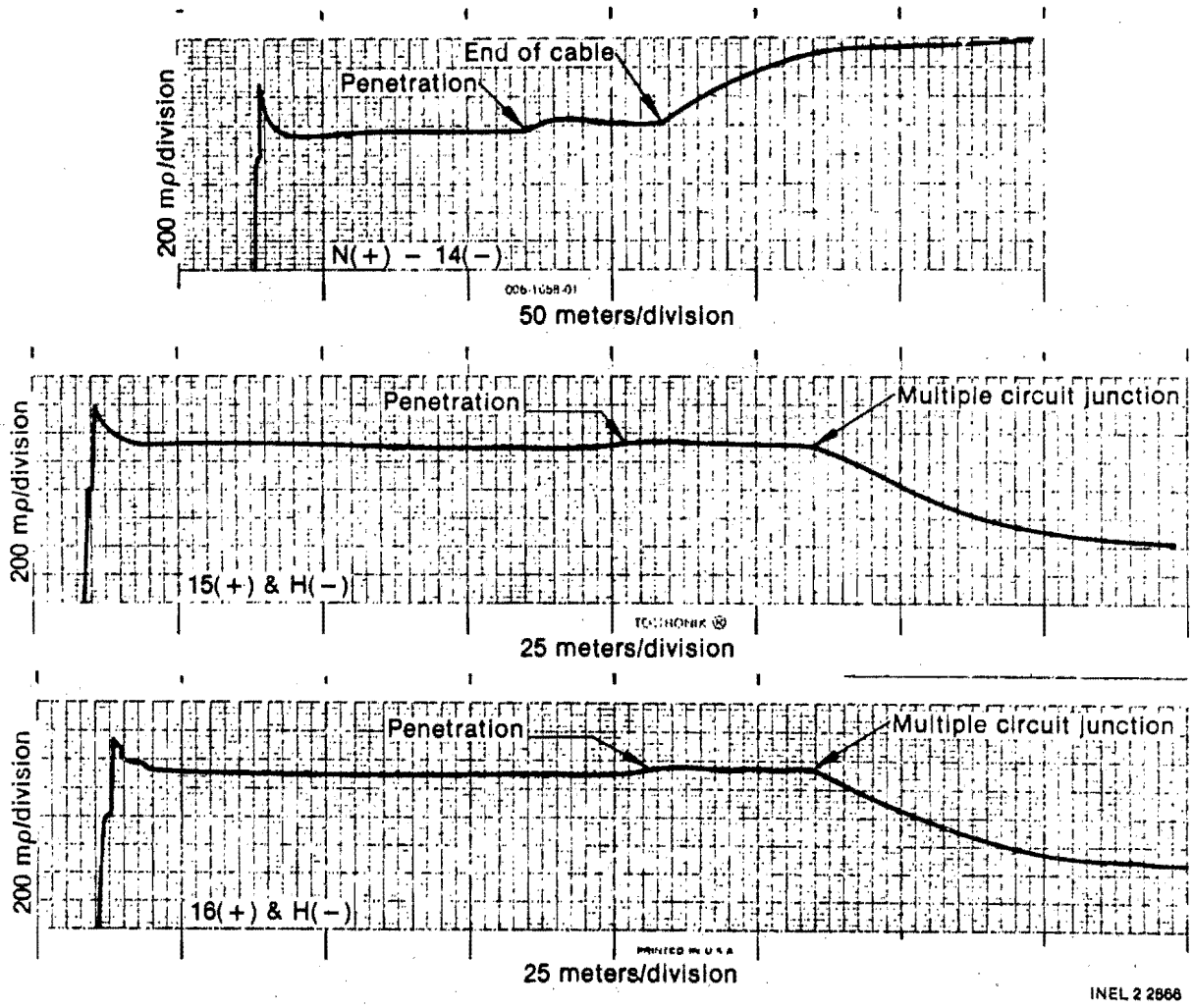

Figure 10. Pre-gross-decontamination TDR traces of AH-V6 circuit.

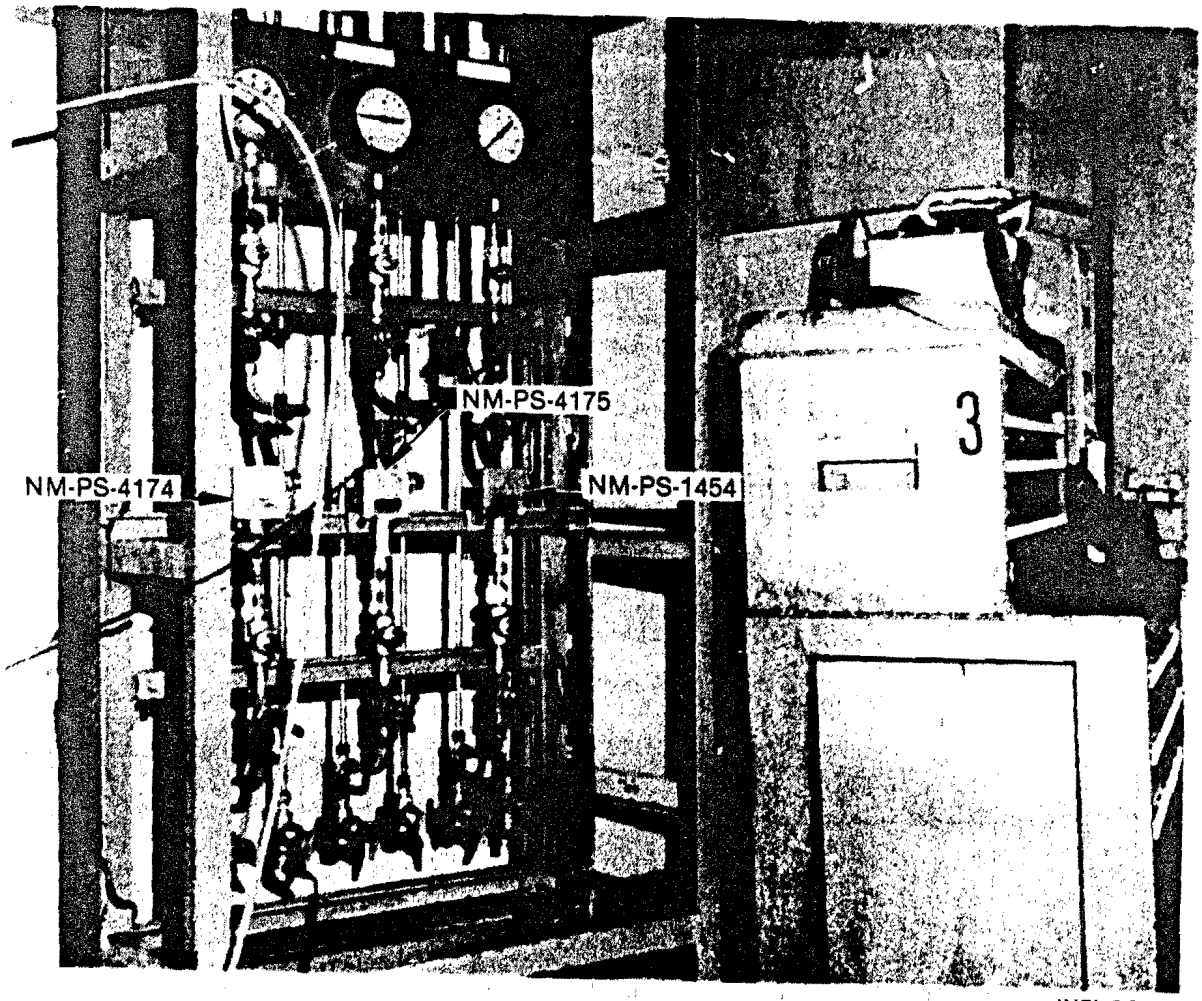

INEL 2 2597

Figure 11. Instrument Rack 432 showing pressure Switches NM-PS-1454, -4174, and -4175.

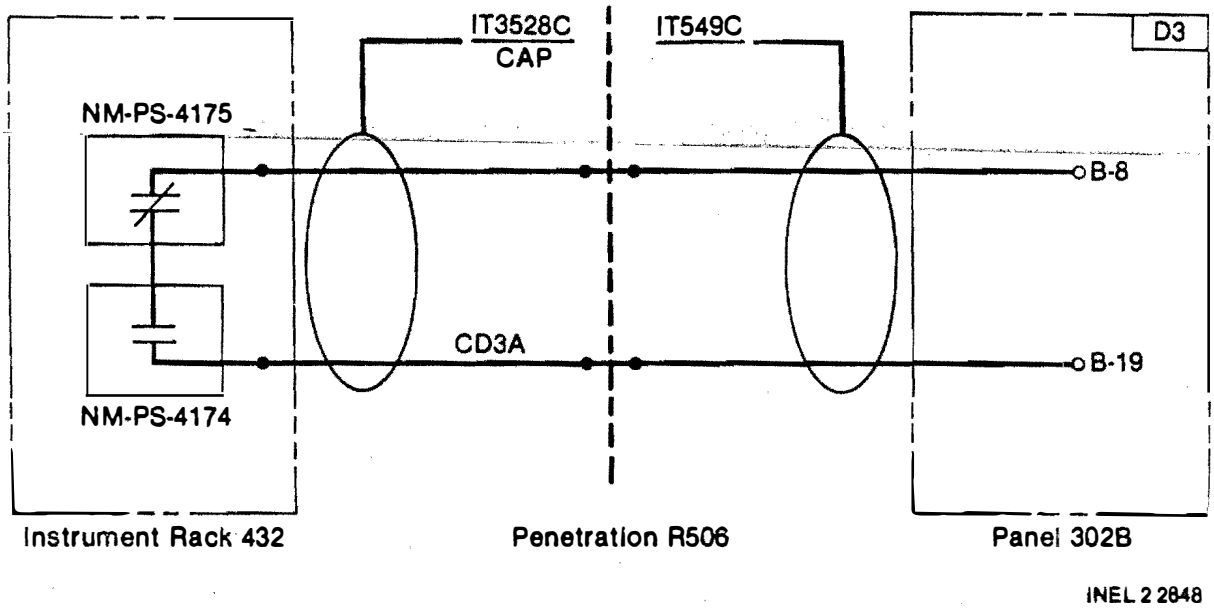

Figure 12. Wiring diagram of NM-PS-4174 and -4175.

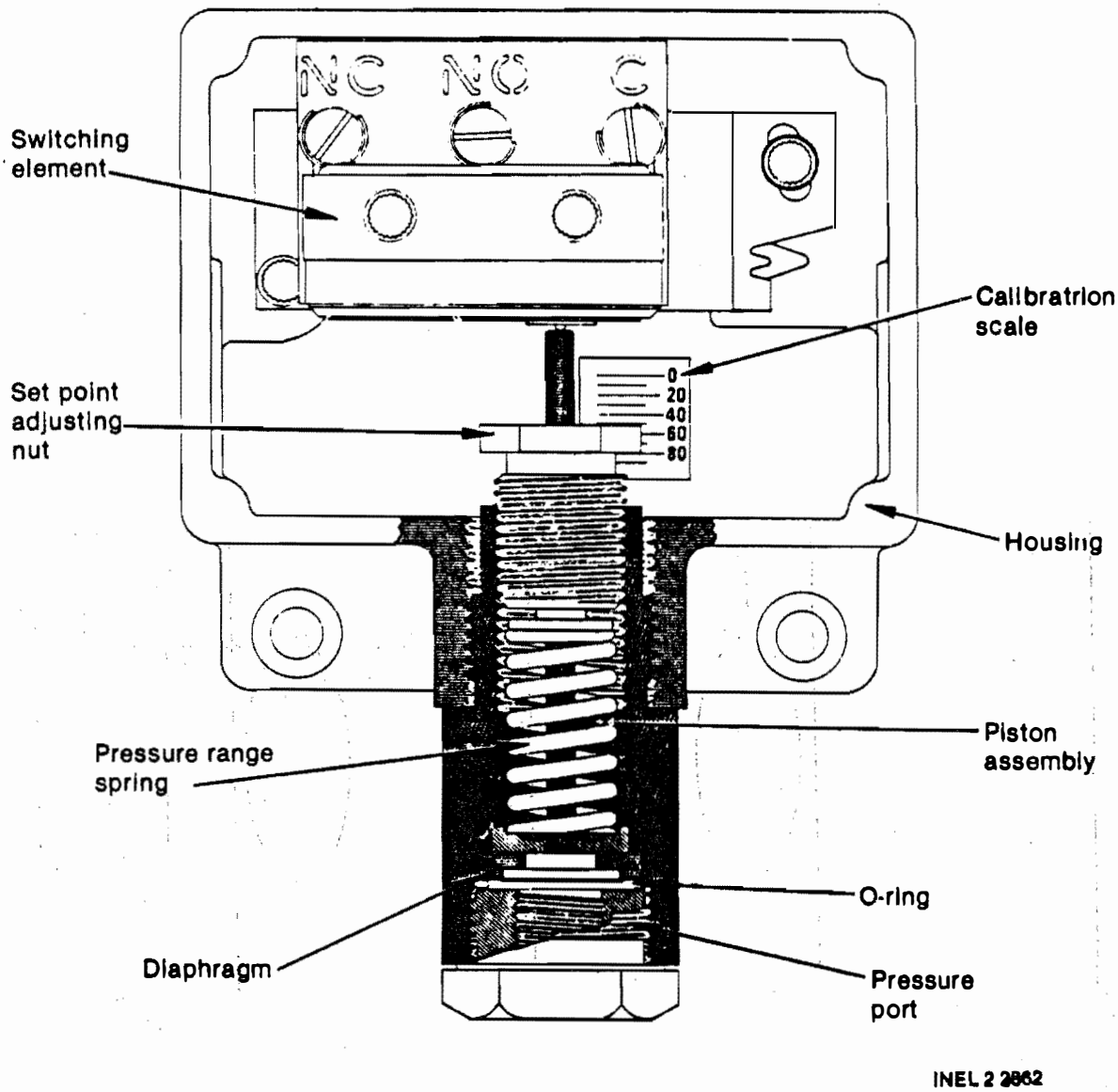

Figure 13. Cutaway view of a Static-O-Ring pressure switch.

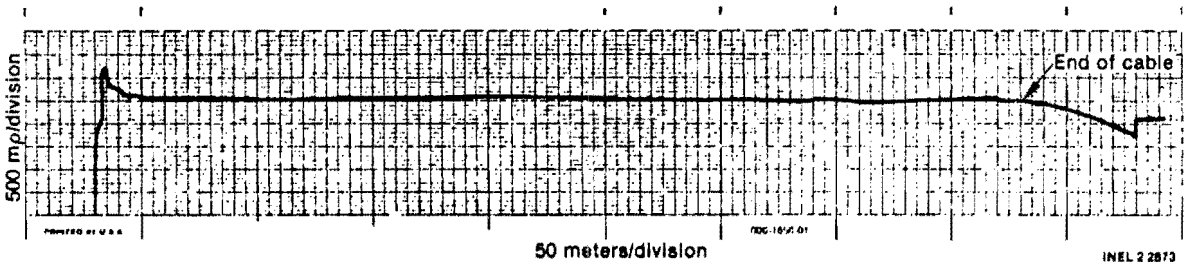

Figure 14. Pre-gross-decontamination TDR trace of NM-PS-4174 and -4175.

During the test, the known system pressure was 0 psig. At this pressure, the contact of NM-PS-4174 should have been open and NM-PS-4175 closed. As expected, NM-PS-4175 was closed since its setpoint is 150 psig on increasing pressure. NM-PS-4174 has a setting of 1.65 psig on increasing pressure and resets at 1.5 psig on decreasing pressure. The condition of NM-PS-4174 implies that it is either out of calibration or its contact is fused closed. Insulation resistance and TDR measurement disclosed no insulation breakdown on either the cable, termination, or the switching elements.

Reactor Coolant Pump Motor Switches

RC56-PS1, RC58-FS1, RC59-FS1, RC60-LS1, and -LS2 are part of the reactor coolant pump Motor RC-P-1A lube oil instrumentation and provide input to the unit computer. RC56-PS1 is a Barksdale sealed piston pressure switch that furnishes the permissive signal when the oil lift pump discharge pressure is adequate for the operation of the reactor coolant pump motor. RC58-FS1 and RC59-FS1 are flow switches made by McDonnell and Miller and are actuated by a paddle device. RC58-FS1 monitors the oil flow through the oil cooler and RC59-FS1 monitors the oil flow to the backstop. RC60-LS1 and -LS2 are Static-O-Ring pressure switches used as level switches to monitor the oil level in the upper reservoir. Each level switch has two sets of SPDT switching elements. RC60-LS1 actuates on high level and RC60-LS2 actuates on low level. The lube oil instruments are electrically connected to the unit computer interface cabinet by Cables H190I and H291I, as shown in Figure 15. Cables H291I and H190I are constructed as follows. They are a 6-pair, 17 AWG stranded conductors, insulated with silicon rubber, twisted in pairs, and jacketed with asbestos braid.

RC56-PS1, RC58-FS1, RC59-FS1, RC60-LS1, and -LS2 were statically tested using one procedure. The dc resistance, inductance, and capacitance measurements across the switch contacts revealed that RC58-FS1 is open and RC56-PS1, RC59-FS1, RC60-LS1, and -LS2 are closed. The dc resistances of 5.02 to 5.17 ohms measured on the "CLOSED" switches agree closely with the expected maximum value of 5.14 ohms.

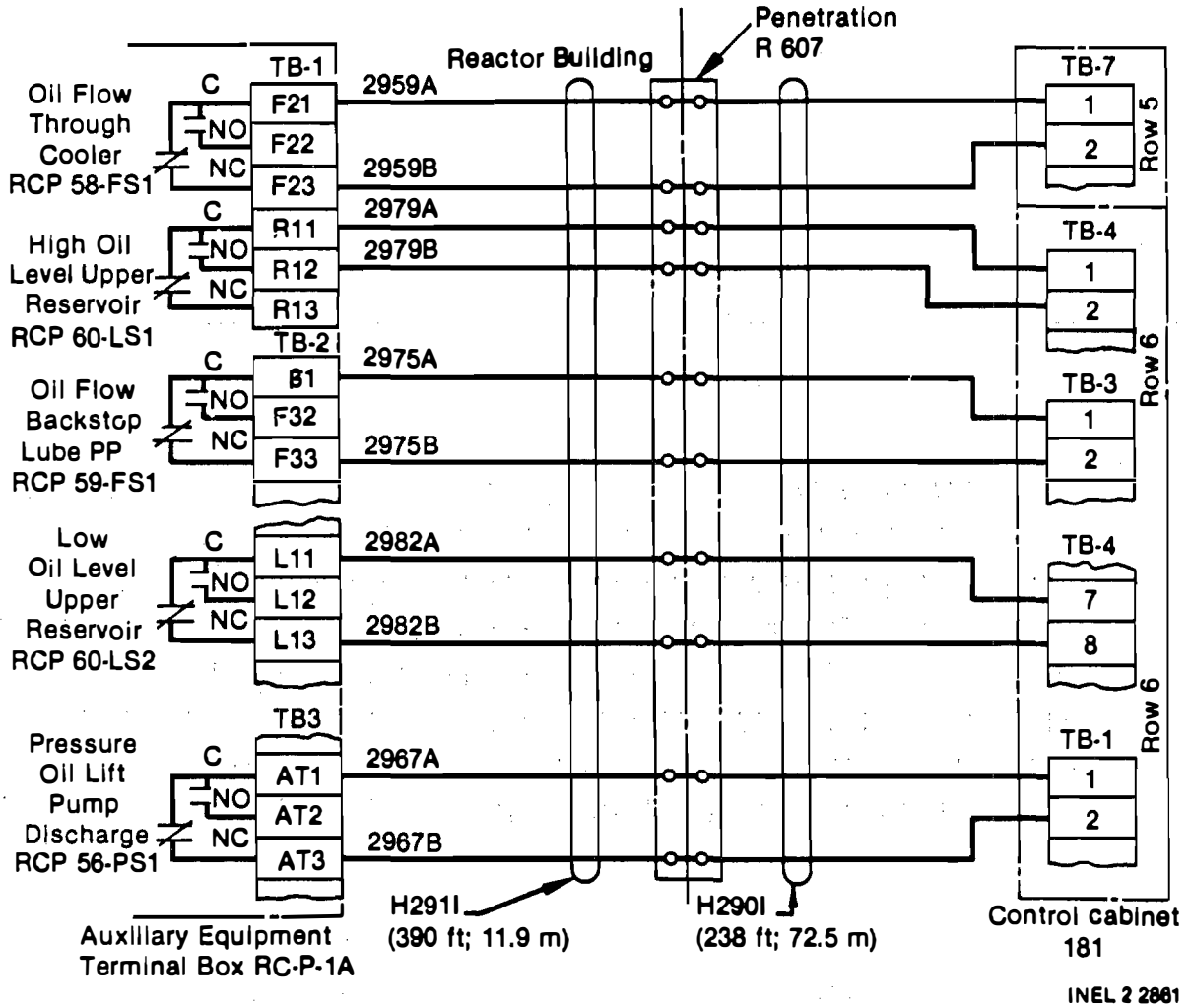

Figure 15. RC-P-1A lube oil instruments interconnection wiring diagram.

The closed state of RC56-PS1 and RC59-FS1 is as expected--indicative of their normal state. The closed contacts of RC60-LS1 and -LS2 indicate that both devices are in the alarm state, signifying a high and low oil level condition in the RC-P-1A motor upper reservoir. Obviously, the two alarm conditions cannot occur simultaneously, implying that one or both of the level switches must be indicating incorrectly. The lack of information on the true status of the oil level precludes the positive identification of the faulty device or devices.

The open state of RC58-FS1 indicates there is oil flow through the oil cooler. However, since there was no oil flow when the measurement was made, the switch should have been closed. The open state of the device implies that it did not return to its normally closed position or a high resistance buildup occurred on the switching element contacts.

The TDR measurements made on each pair of wires shown in Figures 16 through 20 exhibited an unexpected impedance mismatch somewhere in the middle of Cable H291I. The pattern of the mismatch appears to be characteristic of a wet cable. The traces also showed the entire length of Cable H291I. The pattern of the corresponding termination of each wire pair supports the data on the dc resistance measurements.

The insulation resistance measurements which were obtained using a low excitation signal instrument (Fluke 8050A) measured a low of 1.3 megohms to a high of 8.57 megohms. These values were considerably lower than expected notwithstanding the fact that a low excitation voltage of approximately 1.63 V was used. It appears from the insulation resistance and TDR data that the insulation may have suffered a fault, such as water leaching through the insulation.

Vibration Switches

RC67-VS1, -VS3, and -VS4 are vibration switches mounted on reactor coolant pump Motors RC-P-1A, -1B, and -2B, respectively. The vibration switches are Robertshaw Model 366. They actuate when subjected to

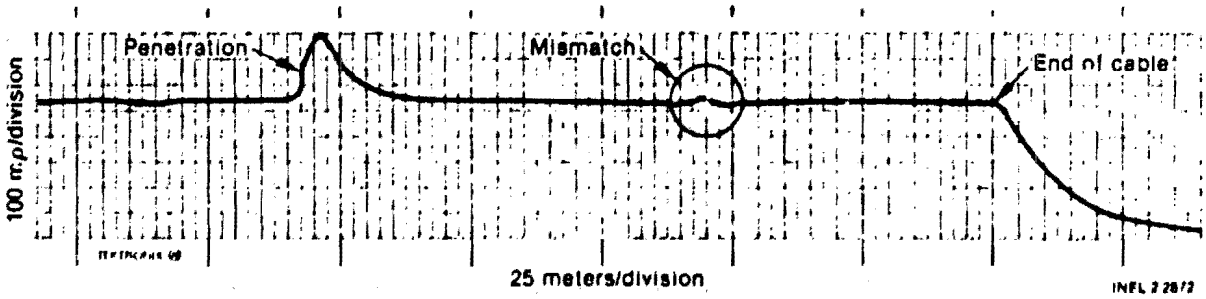

Figure 16. Pre-gross-decontamination TDR trace of RC56-FS1.

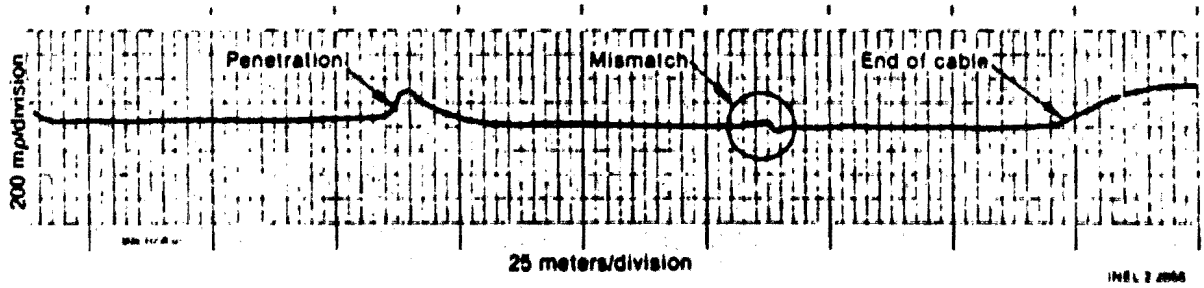

Figure 17. Pre-gross-decontamination TDR trace of RC58-FS1.

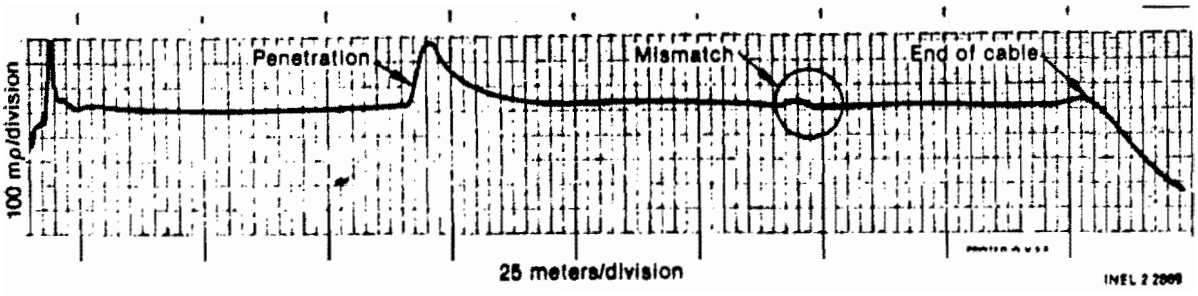

Figure 18. Pre-gross-decontamination TDR trace of RC59-FS1.

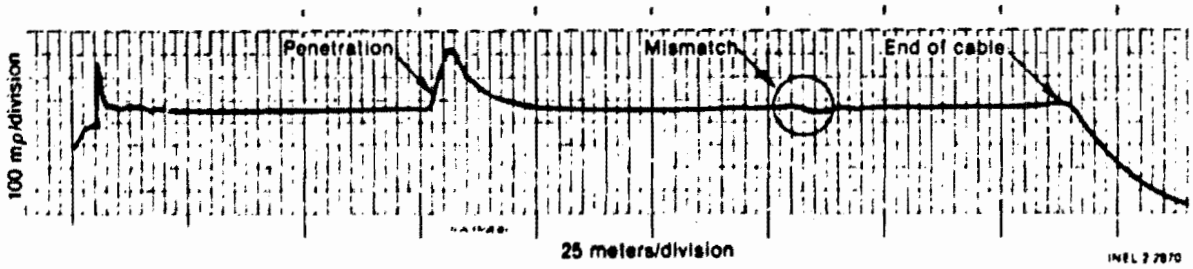

Figure 19. Pre-gross-decontamination TDR trace of RC60-LS1.

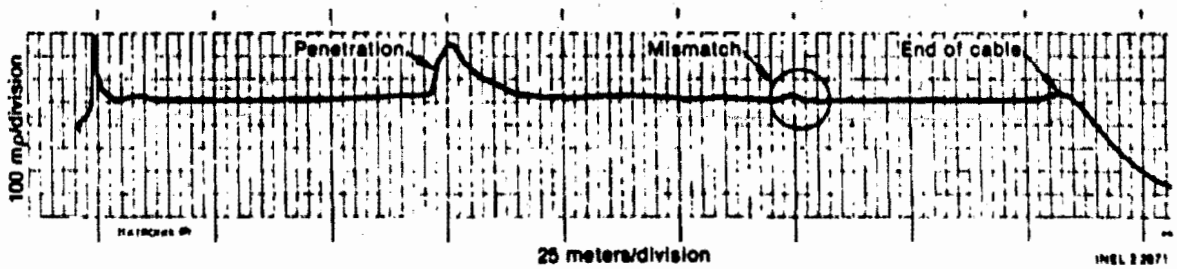

Figure 20. Pre-gross-decontamination TDR trace of RC60-LS2.

abnormally high vibration. When actuated, the devices are mechanically latched in the trip position until released by an integral 125 V dc-operated reset mechanism. The vibration switches are electrically connected to the associated RC pump motor switchgear by the same control cables used for the motor start permissive circuit. These circuits are shown in Figures 21, 22, and 23.

The test of vibration Switches RC67-VS1, -VS3, and -VS4 indicated a very high electrical noise existed on the circuits. However, the available data indicated that Switch RC67-VS1 suffered a break in its reset coil circuit as proven by the dc resistance of 9.8×10^7 ohms. The test data also showed that RC67-VS1 was in the tripped state as indicated by the short circuit across Wires A3VSP and A3VS.

The data obtained on RC67-VS3 and RC68-VS4 indicate that both devices are operational. Both were found in their normal state, operated when energized, and had holding currents of 133 mA and 180 mA. The measured holding currents differ slightly from those expected from the measured dc resistance of 1150 and 1044 ohms and the coil rating of 14 W. The difference may be attributed to the measurement technique and level of accuracy.

Reactor Coolant Pump Motors

Reactor coolant pump Motors RC-P-1A and -2B are 3-phase, 6900 V ac, 9000 hp induction motors manufactured by Allis-Chalmers. A typical reactor coolant pump motor installation and its environmental conditions are shown in Figure 24. These motors are equipped with a set of wye-connected current transformers (CT) used in the motor differential current protection circuit and two sets of current and potential transformers (PT) used for power monitoring. Each motor feeder has two parallel 500 MCM cables per phase. Figures 25 and 26 show the interconnection wiring diagrams of RC-P-1A and -2B, respectively. Both motors experienced a high vibration when operated during the accident recovery.

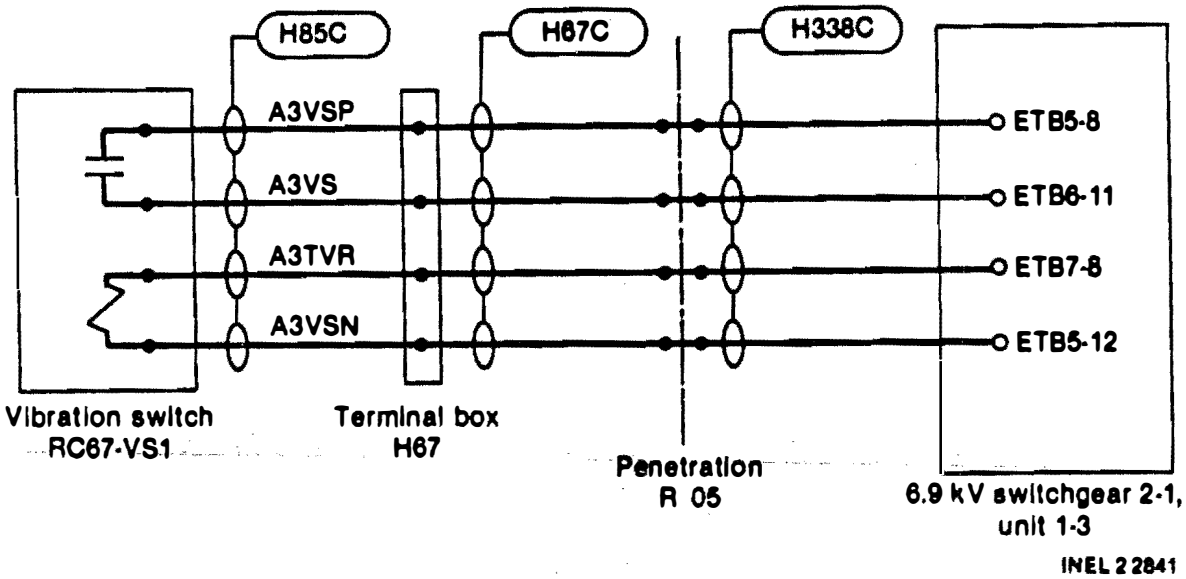

Figure 21. Interconnection wiring diagram of RC67-VS1.

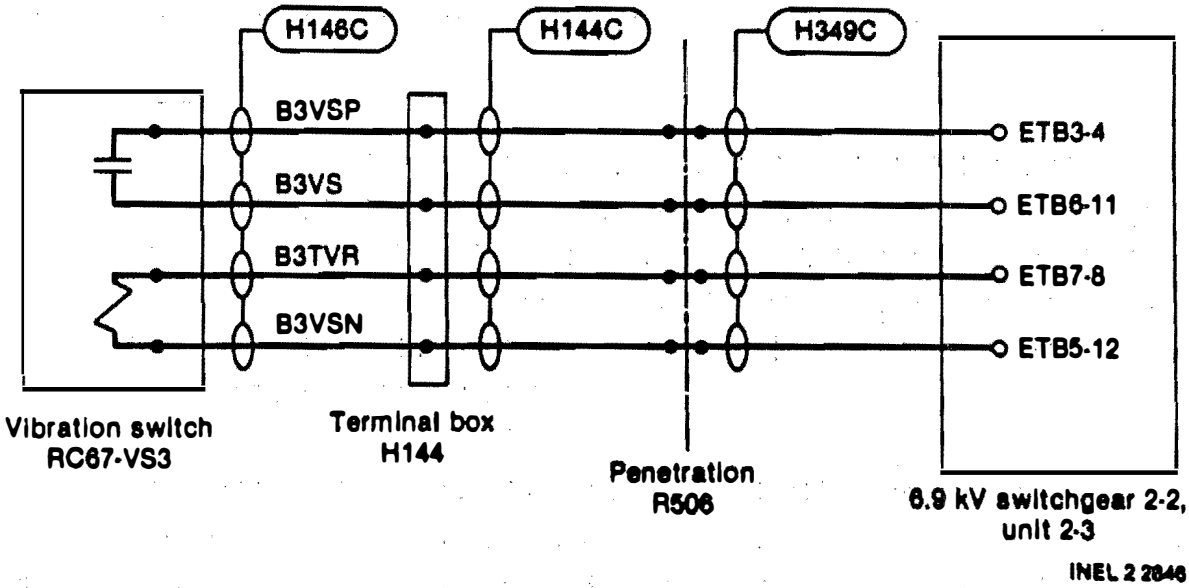

Figure 22. Interconnection wiring diagram of RC67-VS3.

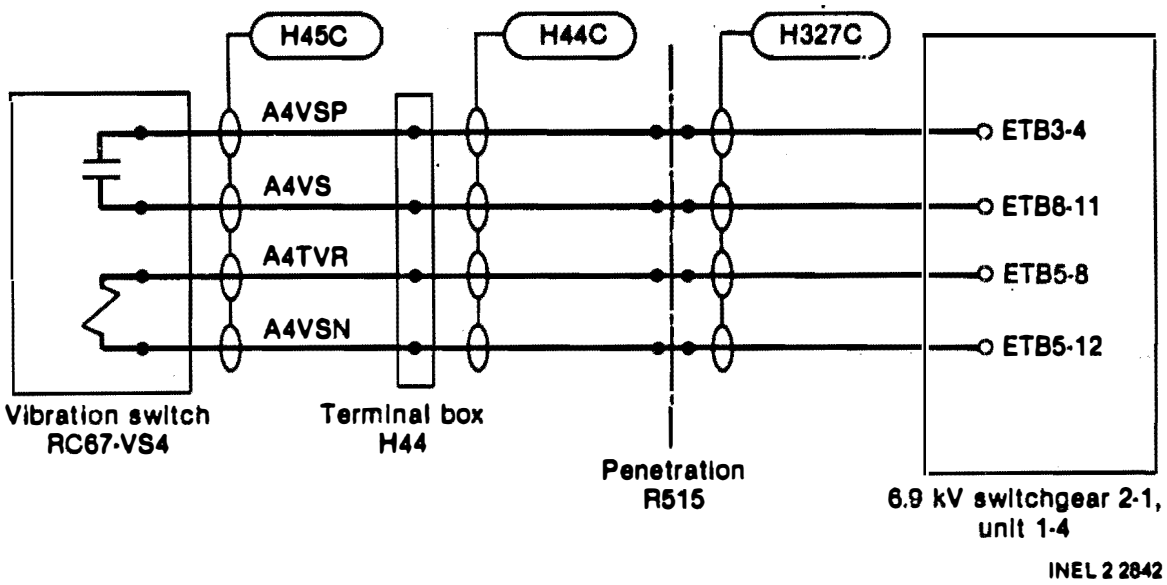

Figure 23. Interconnection wiring diagram of RC67-VS4.

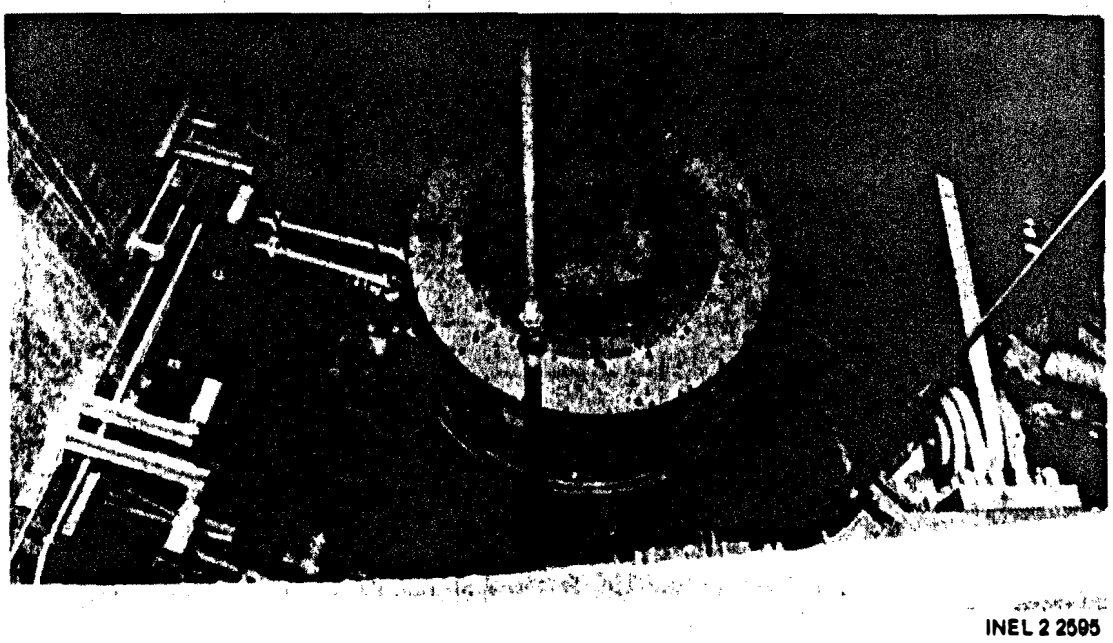

Figure 24. Reactor coolant pump inside D-Ring B.

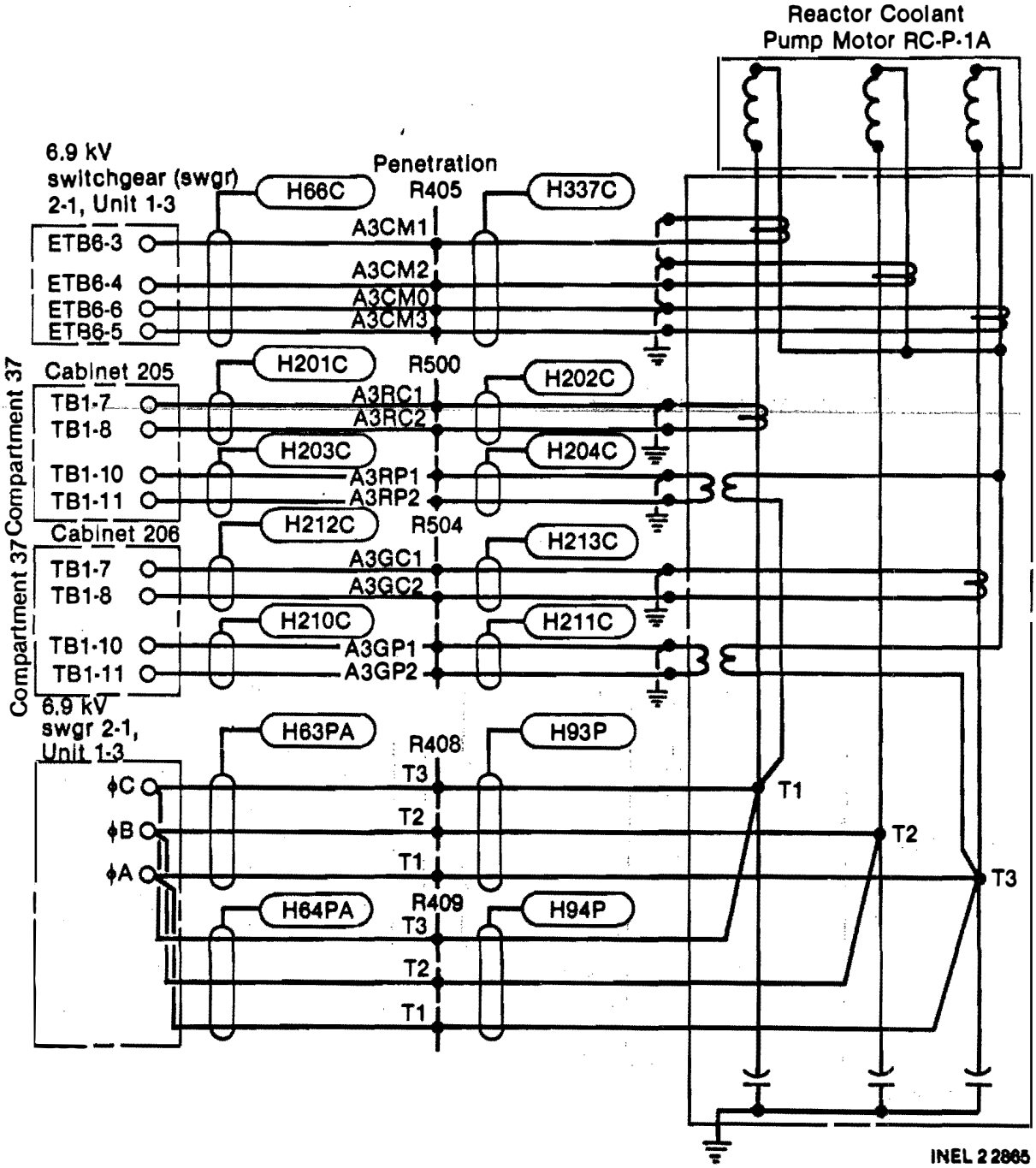

Figure 25. Interconnection wiring diagram of RC-P-1A motor.

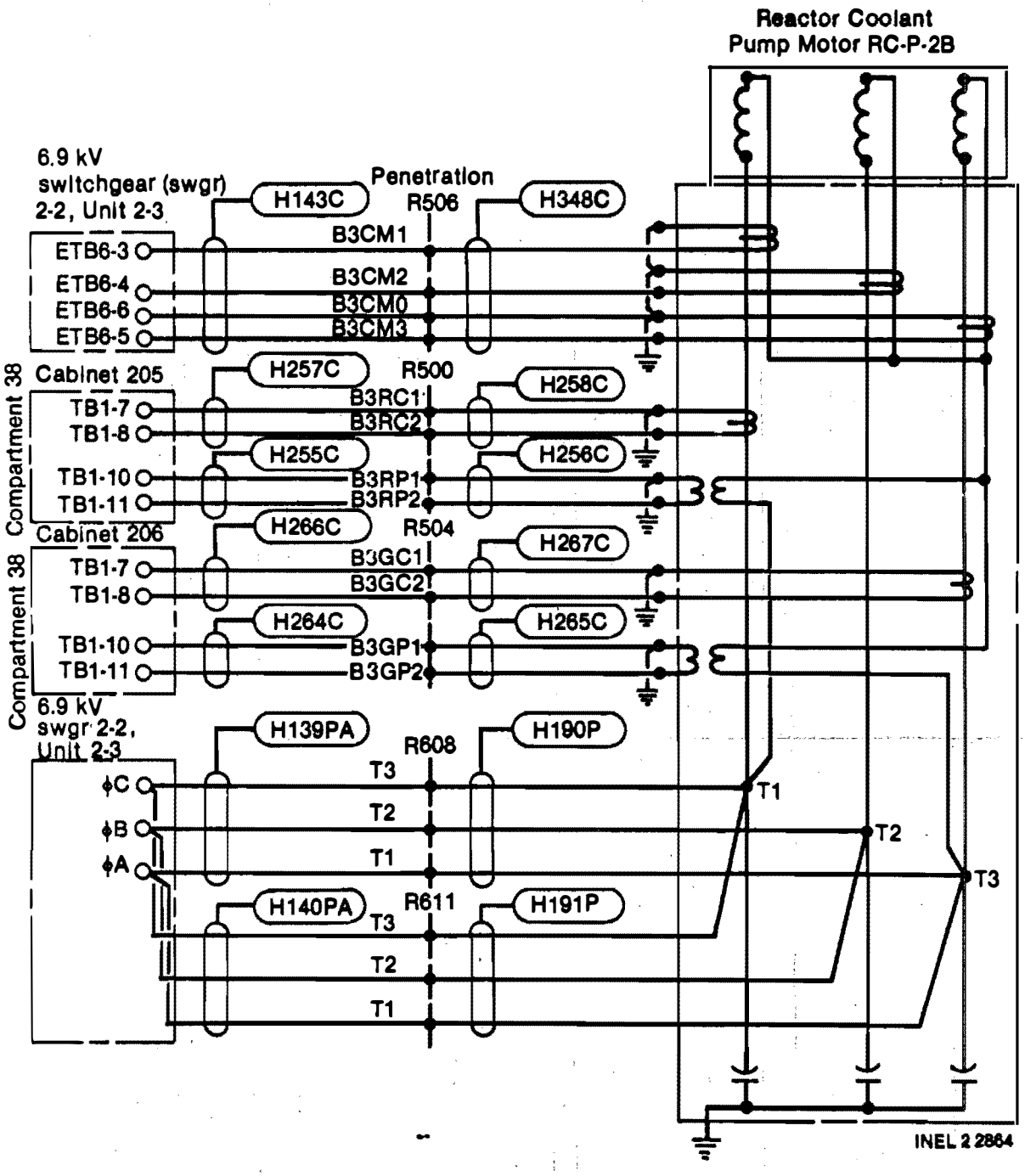

Figure 26. Interconnection wiring diagram of RC-P-2B motor.

Reactor coolant pump Motors RC-P-1A and -2B exhibited an elevated dc resistance across their stator windings of 21 and 38 ohms, respectively. These readings, supported by the TDR measurements shown in Figures 27 through 34 are many times higher than the measured startup value of less than 0.1 ohm.

All the CTs and PTs likewise exhibited abnormally high dc resistance across their windings. Additionally, a differential CT winding of RC-P-1A showed an open circuit. Analysis of the test data revealed that Circuit A3CM1 shown in Figure 28 has a discontinuity in the vicinity of the reactor building electrical penetration R405. One logical explanation of these elevated dc resistances could be the buildup of copper oxide compounds at termination and junction points; however, other causes cannot be totally discounted. The possible loosening of connectors when the motors were operating under a very high vibration level coupled with the high humidity environment could have eventually led to the formation of the copper oxide.

The insulation resistance of RC-P-1A and -2B motors were also observed to be abnormally low. RC-P-1A had a 2.5 megohm insulation resistance and a polarization index of 1.2. RC-P-2B had an insulation resistance of 10 megohms and a polarization index of 1.05. RC-P-1A motor had an insulation resistance well below the minimum required for operation of 7.6 megohms. Both motors, evidently, have wet and/or dirty insulation as evidenced by the low polarization index.

Oil Pump Motors

Backstop lube oil Pumps 2-1A-1 and 2-1B-1 are associated with reactor coolant Pumps RC-P-1A and -1B, respectively. They are driven by 1/2 hp, 1150 rpm, 460 V ac, 3-phase, 60 Hz induction motors. These motors were operated during the accident to support reactor coolant pump operation. Figure 35 shows the equipment interconnection wiring diagram.

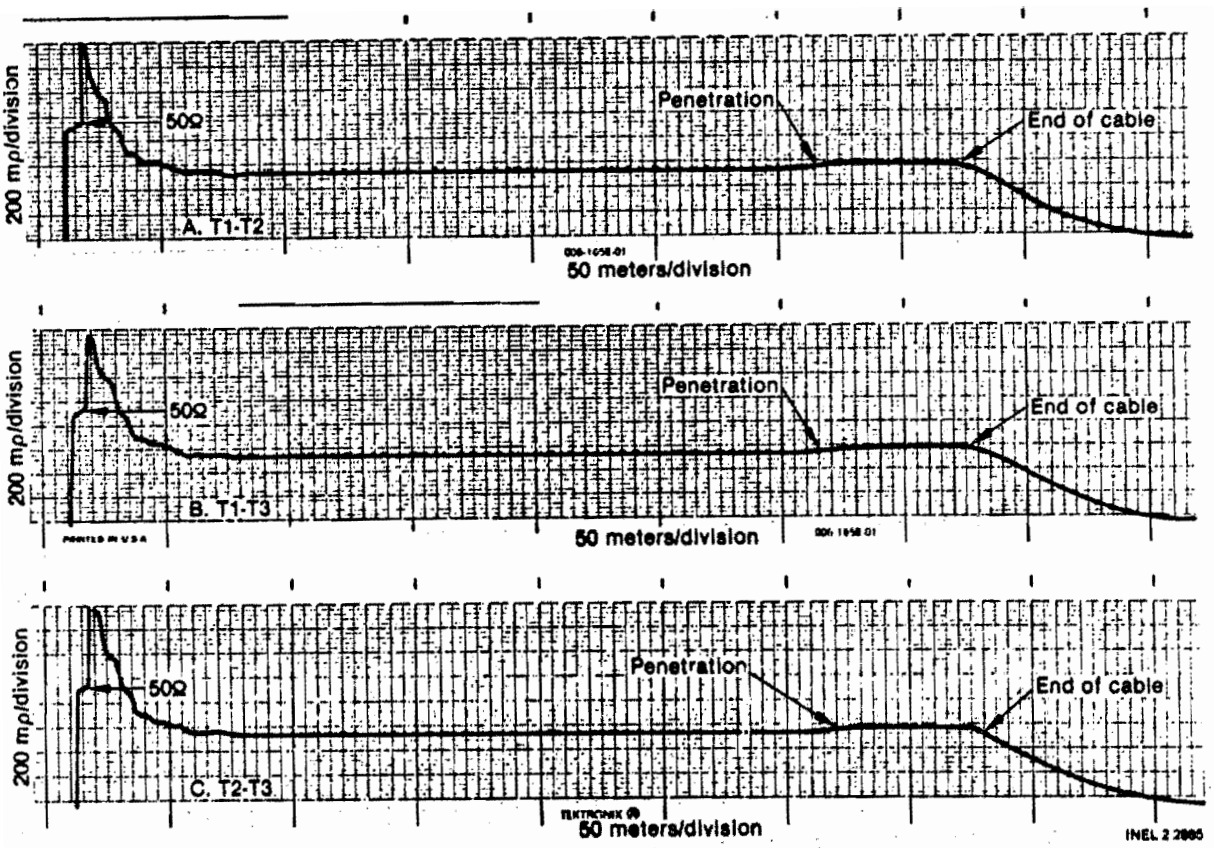

Figure 27. Pre-gross-decontamination TDR trace of the winding of RC-P-1A motor.

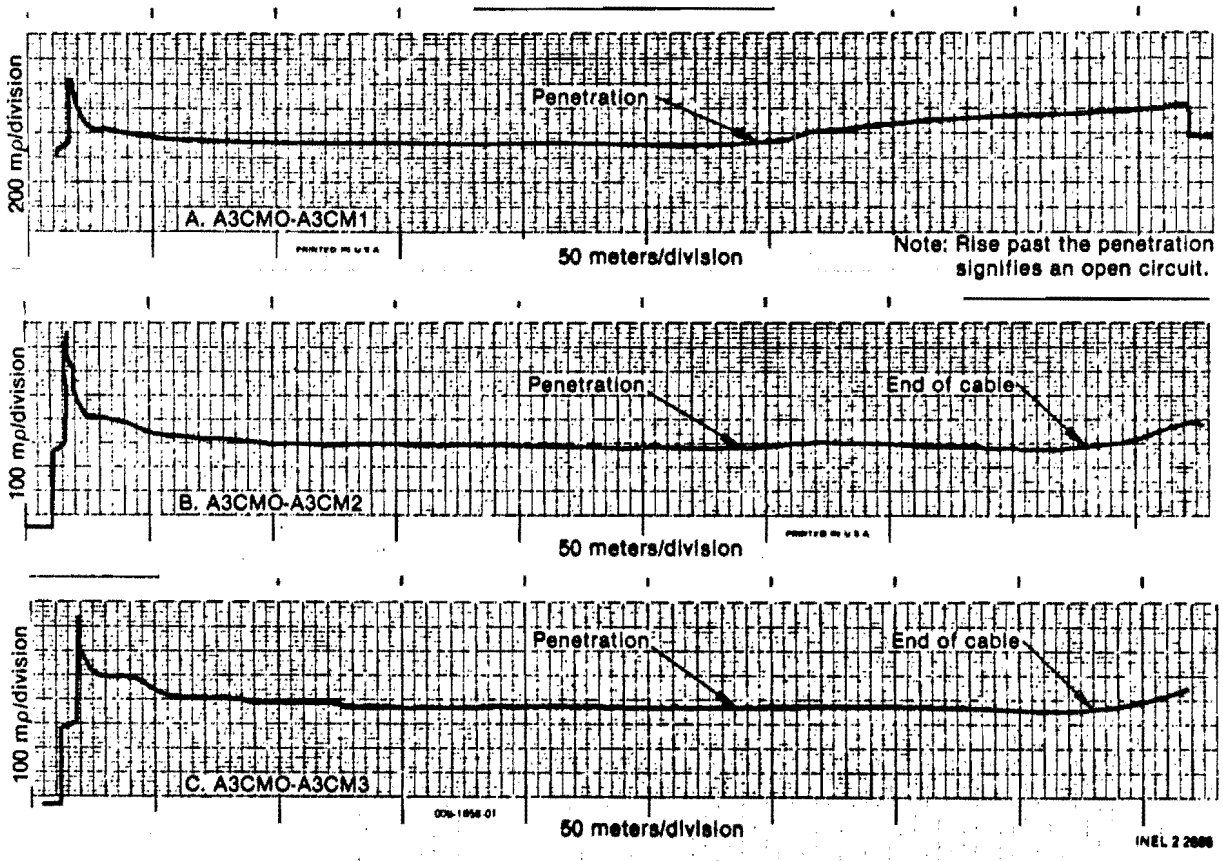

Figure 28. Pre-gross-decontamination TDR traces of the RC-P-1A differential current transformers.

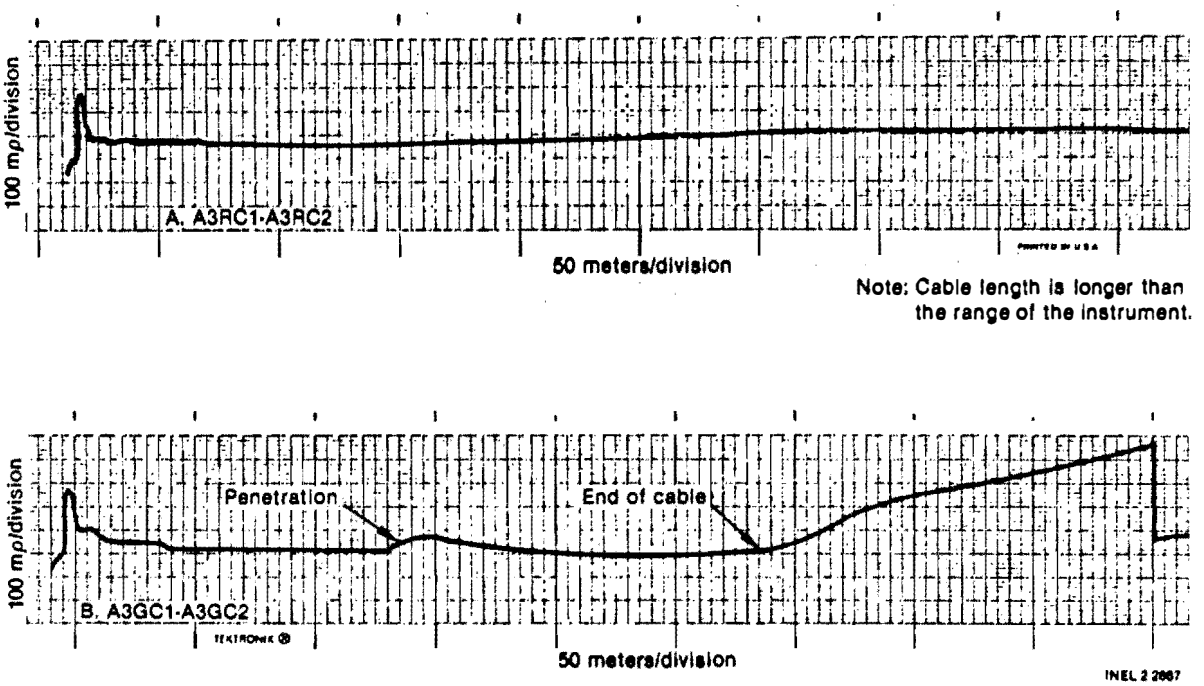

Figure 29. Pre-gross-decontamination TDR trace of the RC-P-1A power monitoring system current transformers.

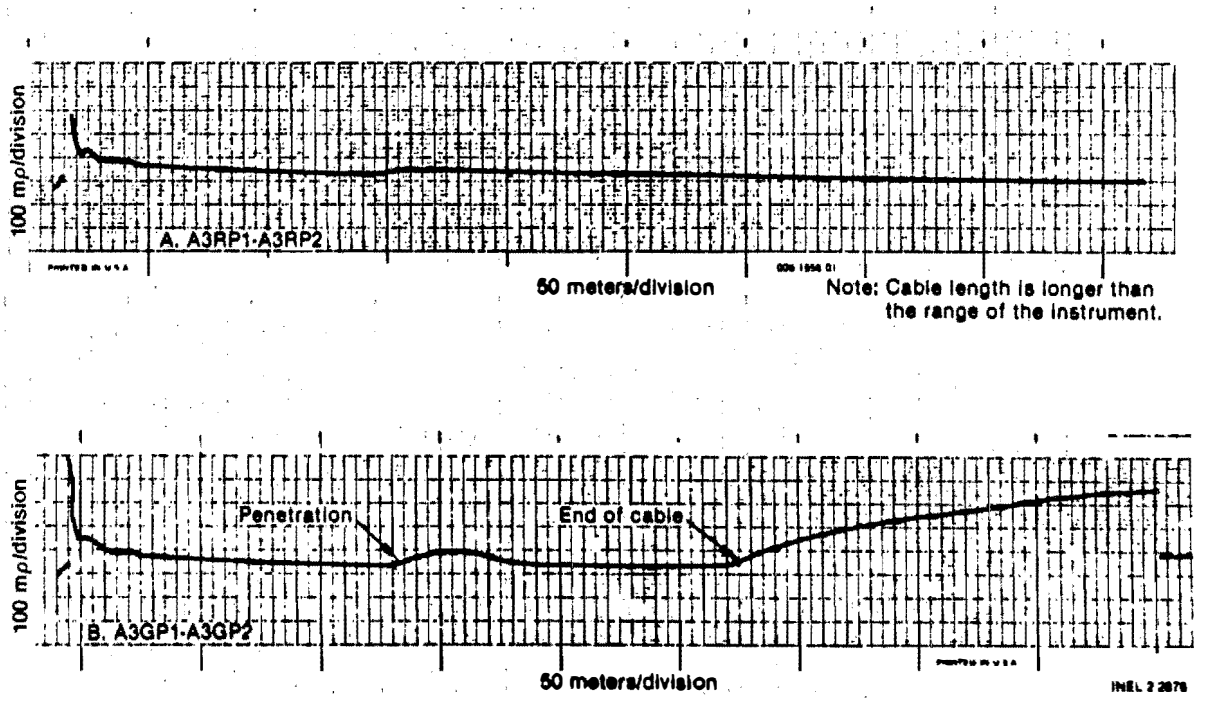

Figure 30. Pre-gross-decontamination TDR trace of the RC-P-1A power monitoring system potential transformers.

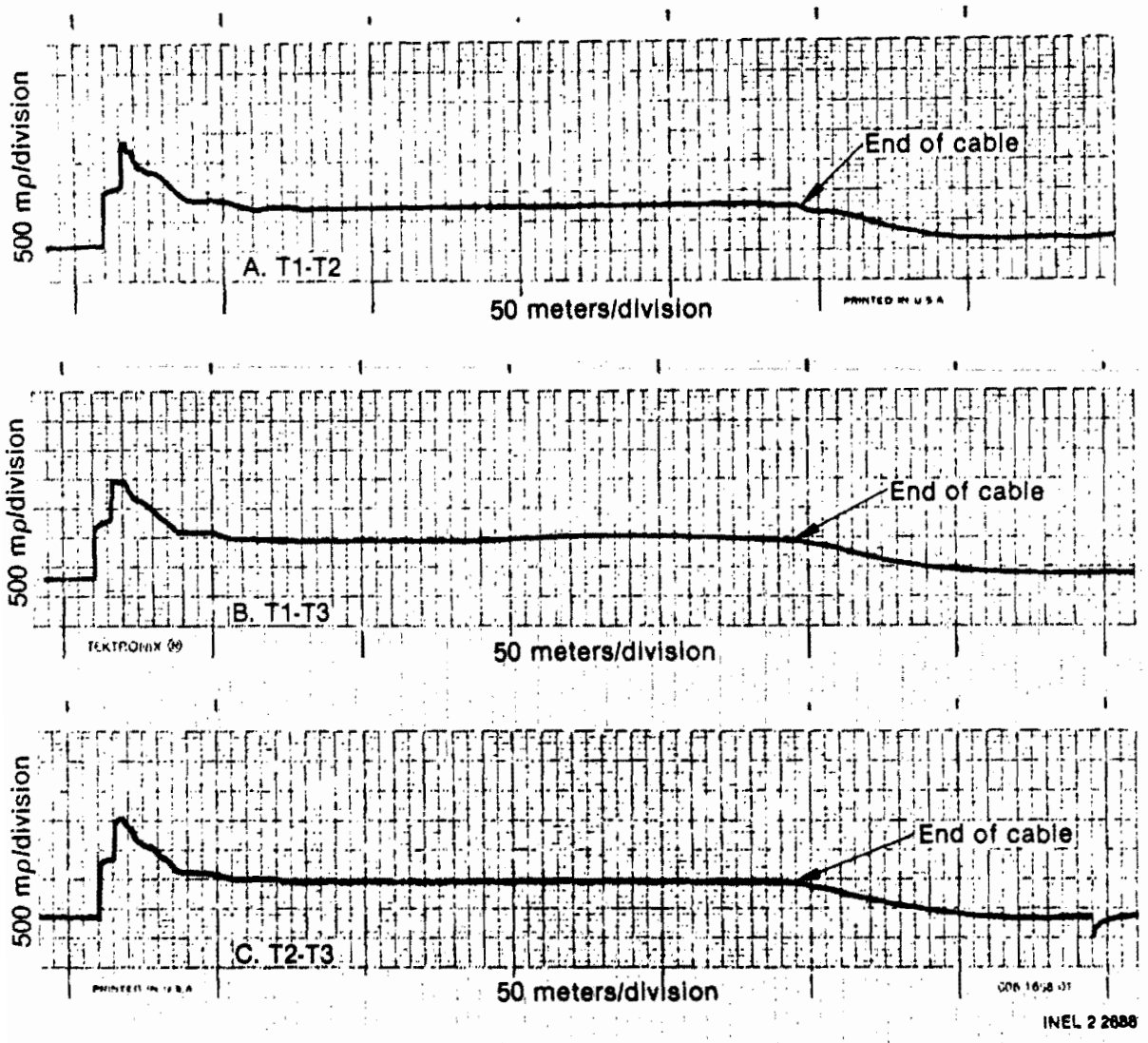

Figure 31. Pre-gross-decontamination TDR traces of the RC-P-2B motor windings.

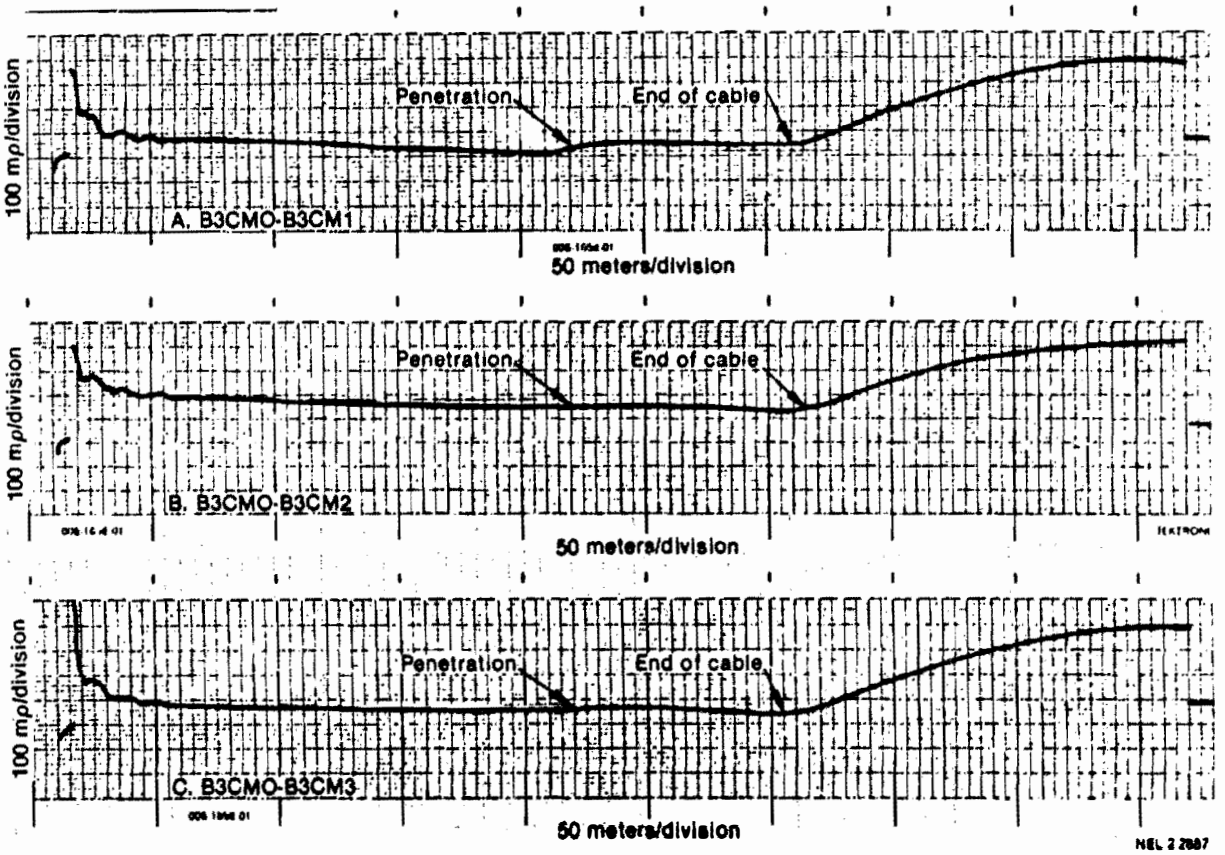

Figure 32. Pre-gross-decontamination TDR traces of the RC-P-2B differential current transformers.

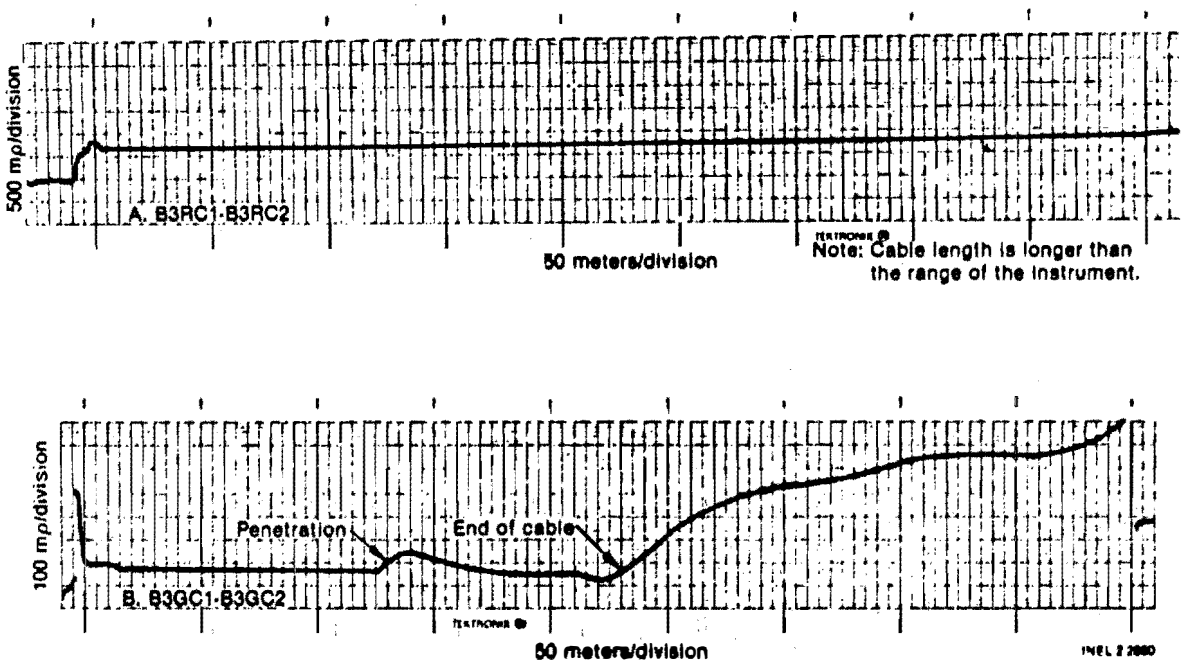

Figure 33. Pre-gross-decontamination TDR trace of the RC-P-2B power monitoring system current transformers.

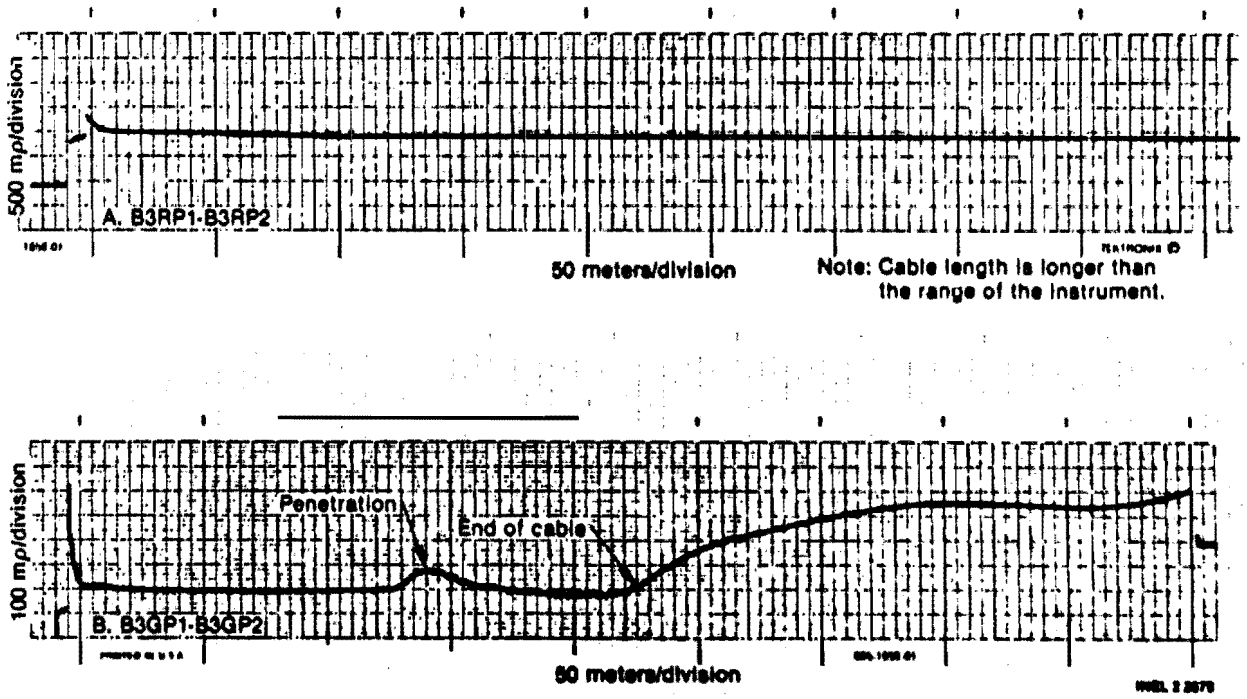

Figure 34. Pre-gross-decontamination TDR trace of the RC-P-2B power monitoring system potential transformers.

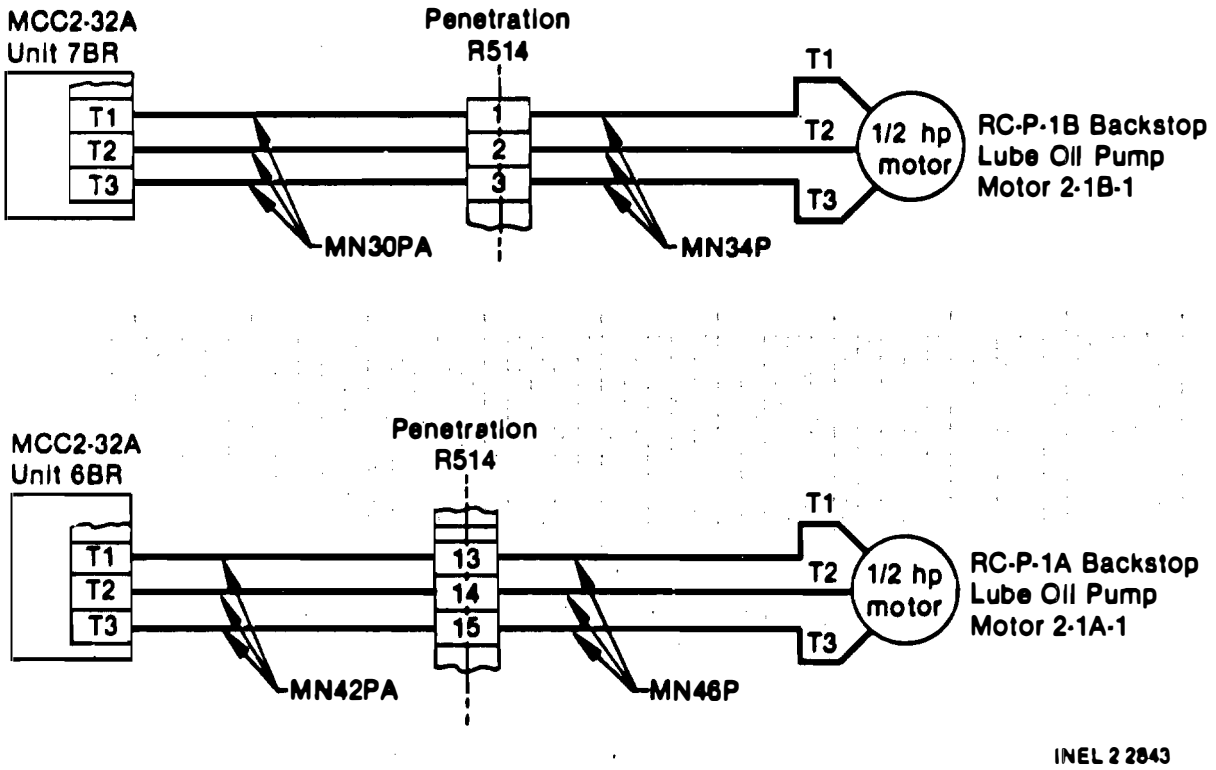

Figure 35. Interconnection wiring diagram of backstop lube oil/pump Motors 2-1A-1 and 2-1B-1.

The tests performed on RC pump backstop lube oil Pumps 2-1A-1 and 2-1B-1 did not provide sufficient information to evaluate the status of the motors. The equivalent series resistance (ESR) was measured instead of the dc resistance. The ESR of Motor 2-1A-1 circuit varied from 10.44 to 10.67 kilohms while 2-1B-1 had a value that varied from 77.8 to 81.8 ohms. These values do not correlate to the dc resistance of 40 ohms made during the startup. The TDR traces shown in Figures 36 and 37 agree with that expected from a high inductance termination.

The insulation resistance of both motors was unexpectedly high, approximately 5×10^{10} ohms for 2-1A-1 and 3.4×10^{10} ohms for 2-1B-1, while their polarization indexes were low, approximately 1.06 for 2-1A-1 and 1.0 for 2-1B-1. These data indicate that the insulation is good but could be wet or dirty.

Oil Lift Pump Motors

The backup high pressure oil lift pumps associated with reactor coolant pump Motor RC-P-1A and -2B are 10 hp, 1750 rpm, 250 V dc, shunt-wound motors manufactured by Allis-Chalmers. These motors were also operated to support the operation of the associated reactor coolant pump motor during the accident recovery. Their interconnection wiring diagrams are shown in Figures 38 and 39.

Both pump motors, which had an armature dc resistance of 2 ohms during startup, exhibited an abnormally high dc resistance across the armature and field windings during the in situ test. RC-P-1A backup oil lift pump motor has an armature resistance of 3.86×10^6 ohms and an open circuit field winding. RC-P-2B backup oil lift pump motor has an armature resistance of 475 ohms and field winding resistance of 230 ohms. The elevated resistance measured on both motors, and TDR measurements shown in Figures 40 and 41, confirmed that the phenomenon was located at the equipment-end of the cable except for the field winding of RC-P-1A backup oil lift pump motor. The discontinuity on RC-P-1A backup oil lift pump motor field winding was located in the vicinity of the reactor building penetration R400. The high

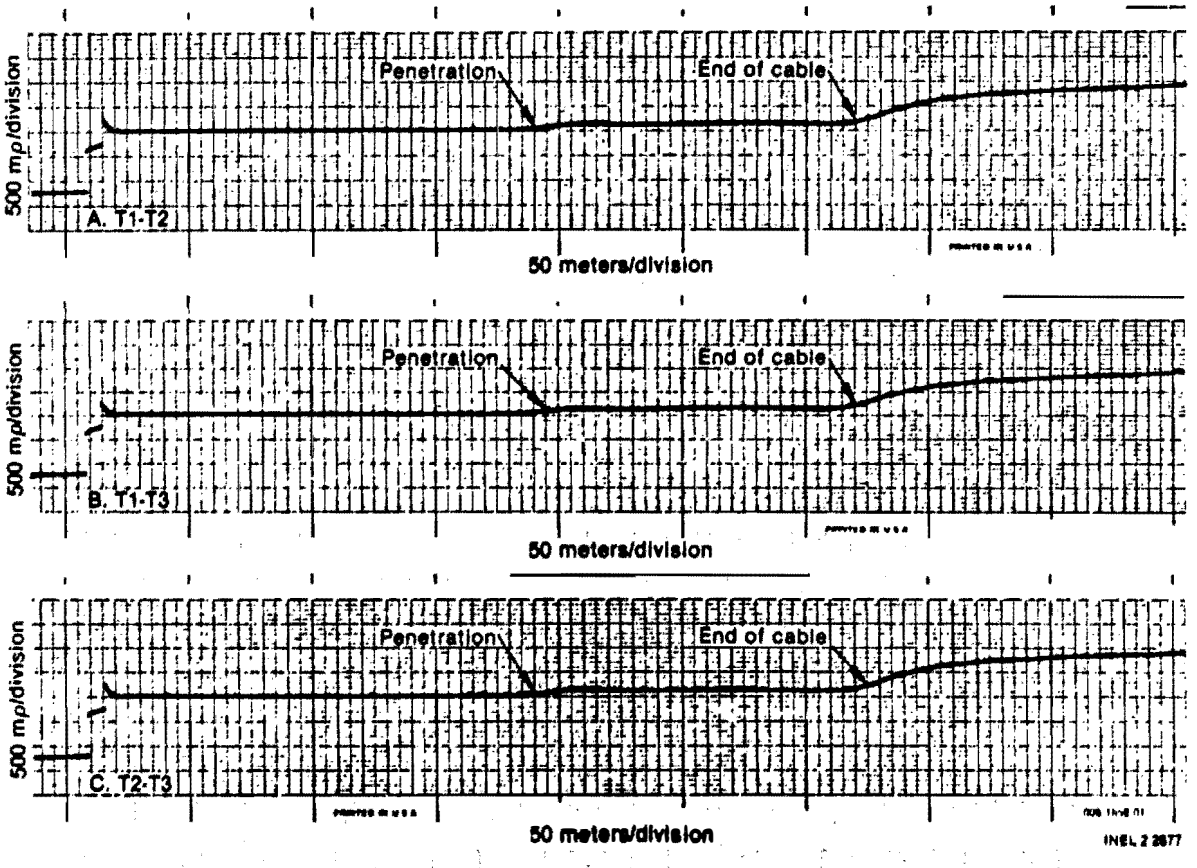

Figure 36. Pre-gross-decontamination TDR traces of the windings of RC-P-1A backstop lube oil pump.

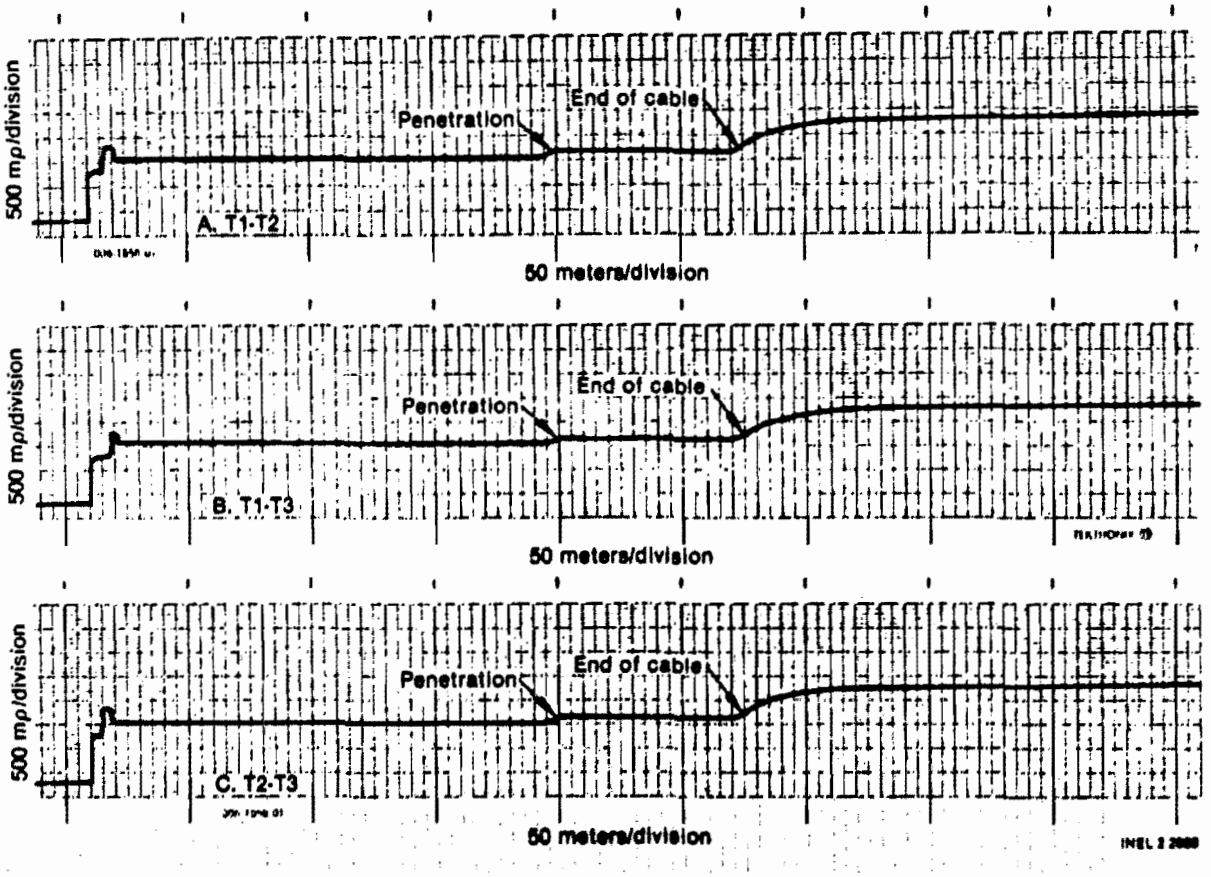

Figure 37. Pre-gross-decontamination TDR traces of the windings of RC-P-1B backstop lube oil pump.

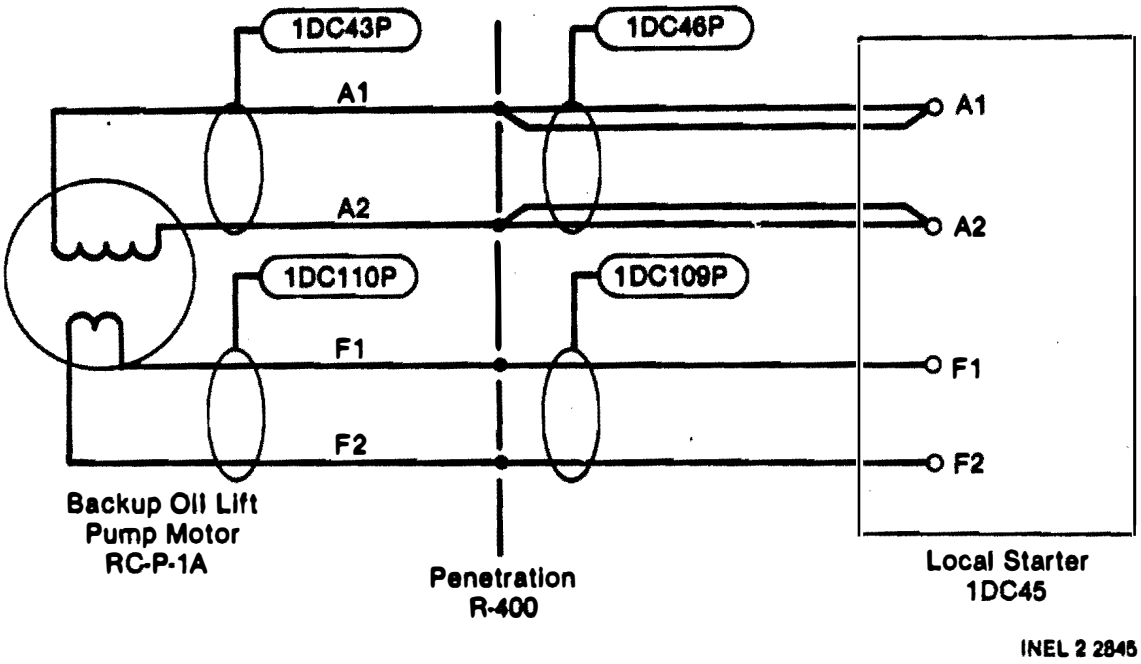

Figure 38. Interconnection wiring diagram of RC-P-1A backup oil lift pump motor.

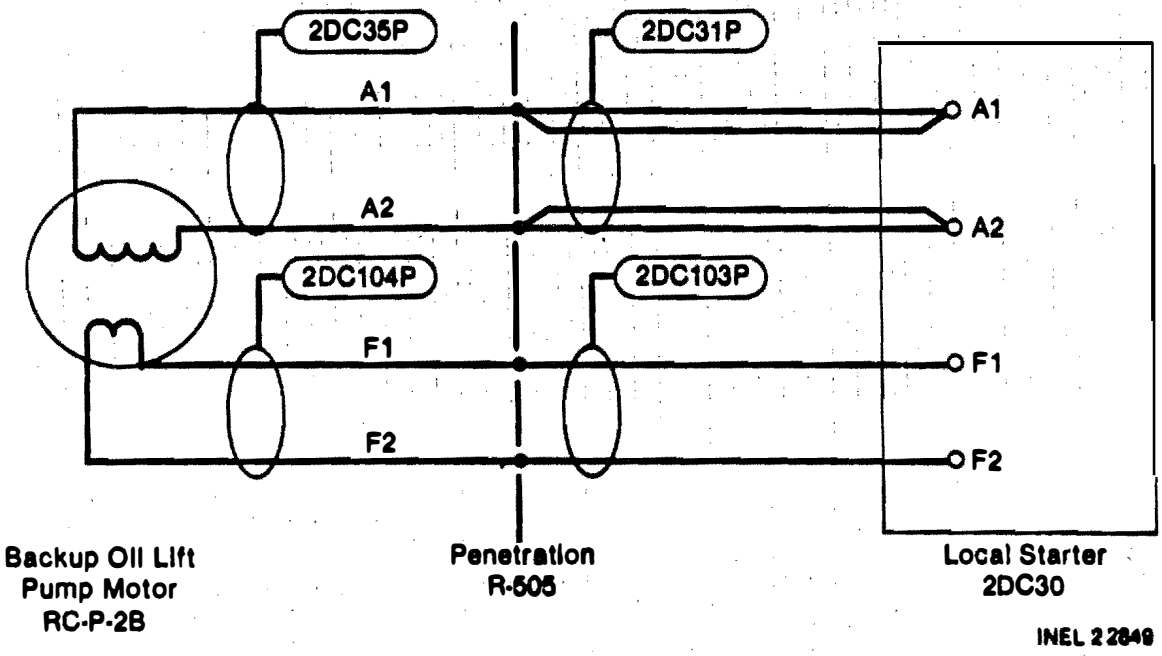

Figure 39. Interconnection wiring diagram of RC-P-2B backup oil lift pump motor.

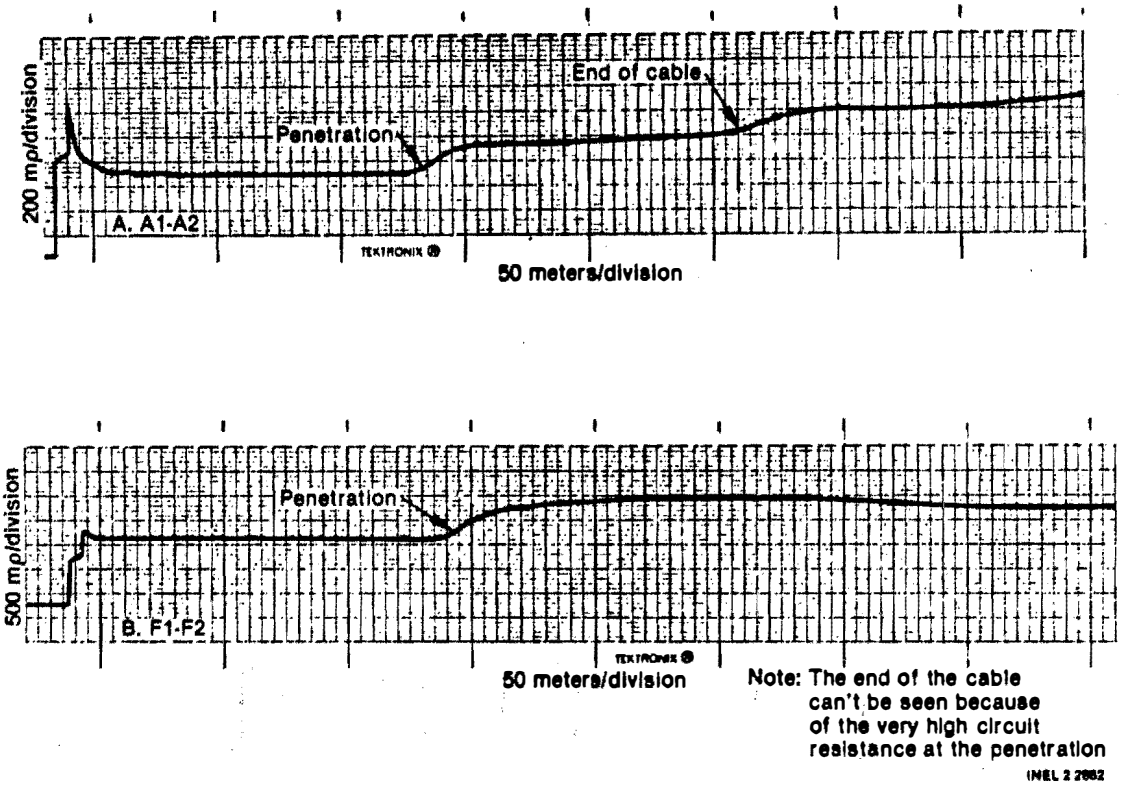

Figure 40. Pre-gross-decontamination TDR signature of the armature and field windings of RC-P-1A backup oil pump motor.

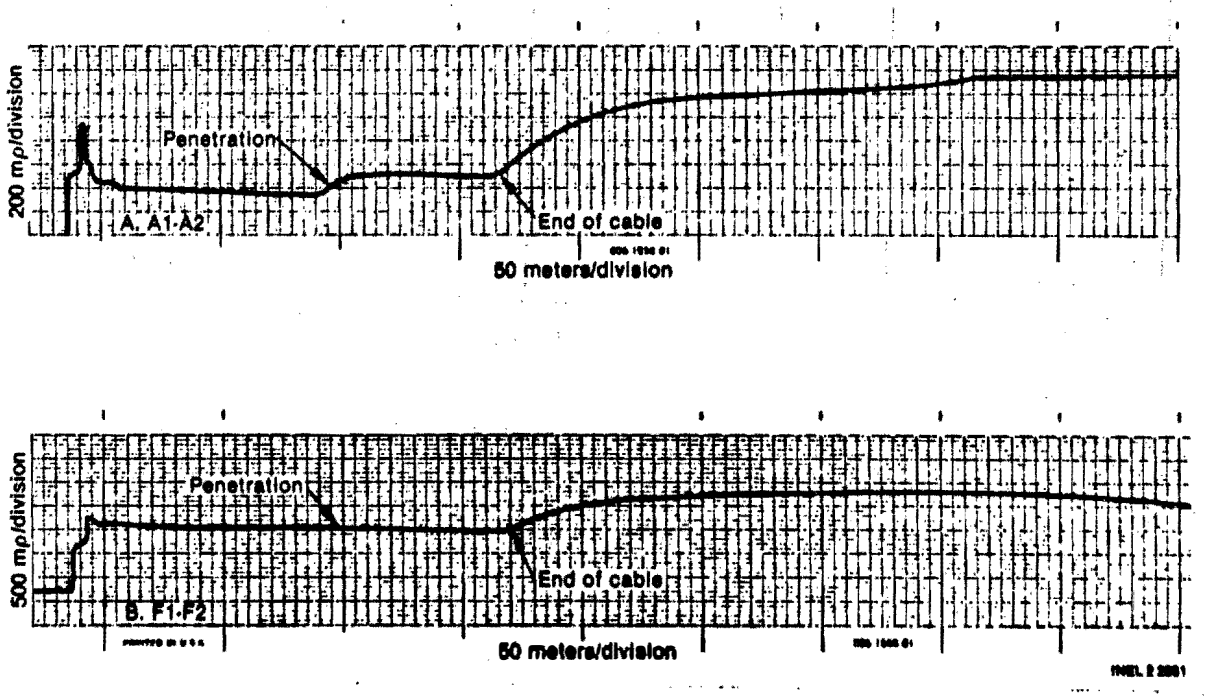

Figure 41. Pre-gross-decontamination TDR traces of the armature and field windings of RC-P-2B backup oil lift pump motor.

resistance observed across the armature windings could be attributed to commutator corrosion. The field winding resistance of RC-P-2B backup oil lift pump motor was within expected values. The high insulation resistances and the polarization indexes of 1.0 indicate good but maybe wet or dirty insulation.

Motor Operated Valves

CA-V1, CF-V1A, NS-V100, RC-V1, and WDL-V271 are Class 1E motor-operated valves. Except for CA-V1, all these valves operated during and after the accident. CF-V1A was closed after the core flooding event and NS-V100 was closed after the reactor coolant pumps were shut down. RC-V1 was operated several times during the accident to initiate the spray in the pressurizer. WDL-V271 was closed after the reactor building sump pumps were stopped.

These valves are equipped with Limitorque operators that are driven by 3-phase, 460 V ac induction motors manufactured by Reliance Electric. The limit and torque switches form an integral part of the operators and have the same basic arrangement and application. Figures 42 through 46 show the interconnection wiring diagrams of CA-V1, CF-V1A, NS-V100, RC-V1, and WDL-V271. Switch Contacts 3 and 7 are used for position indication. Torque Switch 17 opens on mechanical overload in the closing direction and is connected in parallel with limit switch Contact 1 in the "CLOSE" circuit. This arrangement makes the valve to torque-seat closed. Torque Switch 18 opens on mechanical overload in the opening direction and is connected in parallel with limit switch Contact 5 and in series with Contact 4 in the "OPEN" circuit. This arrangement makes the valve position-limited open. The remainder of the limit switch contacts are used for special functions. In addition, a SNAPLOCK switch actuated by the valve stem is used on Valve CF-V1A for position annunciation.

Valves CA-V1, CF-V1A, NS-V100, RC-V1, and WDL-V271 were all subjected to static test measurements. NS-V100 was further tested dynamically. The dc resistances made on the valve operator drive motors agree closely with the values taken during the startup testing. The limit switch positions

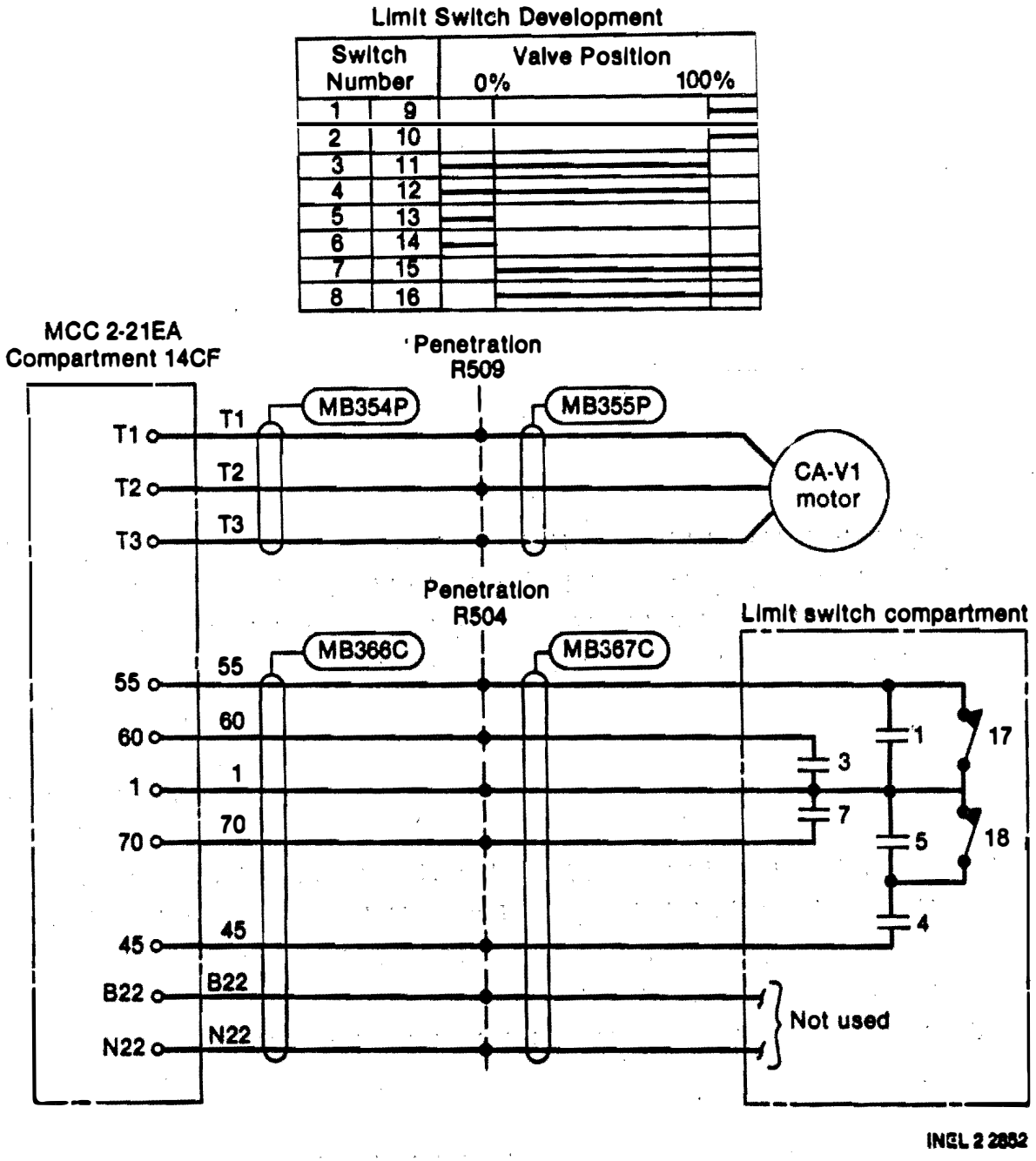

Figure 42. Interconnection wiring diagram of CA-V1.

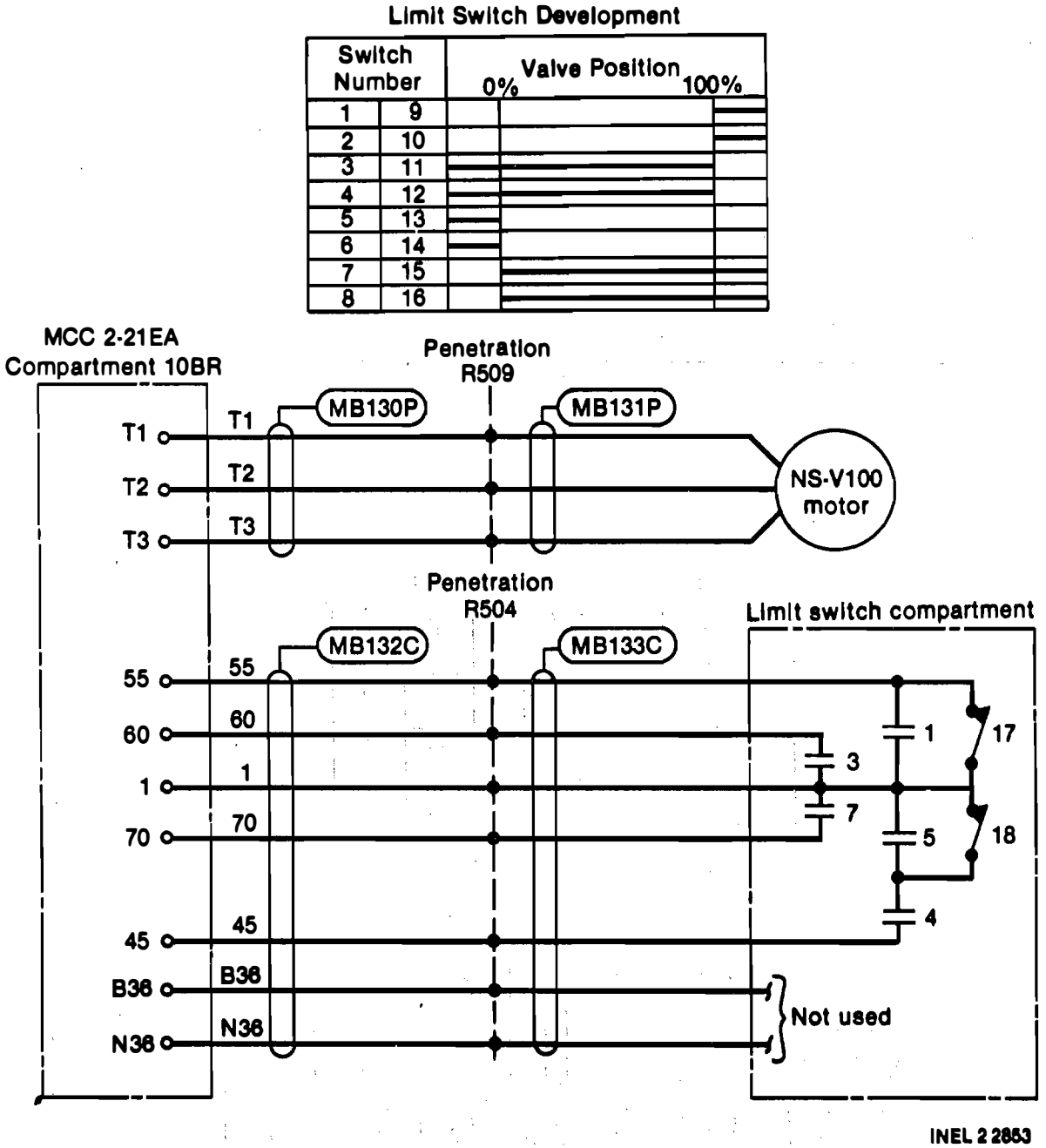

Figure 44. Interconnection wiring diagram of NS-V100.

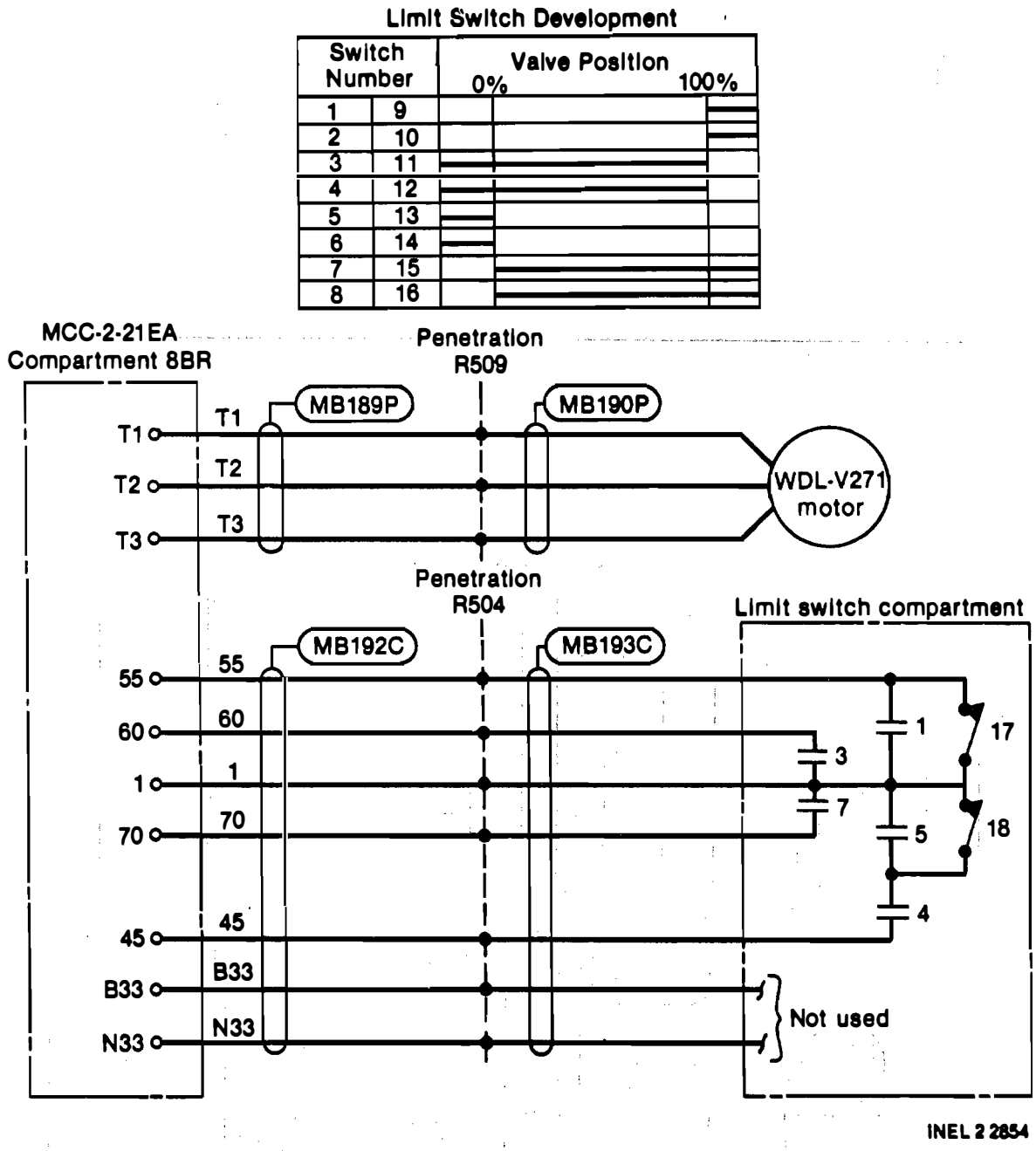

Figure 46. Interconnection wiring diagram of WDL-V271.

TABLE 3. STARTING AND RUNNING CURRENTS OF NS-V100

Test Point	Direction of Operation	Current (amps) Starting	Running
T2	Open	13.5	1.8
T2	Closed	13.5	1.8
T1	Open	12.3	1.9
T1	Closed	11.4	1.7
T3	Open	11.1	2.3
T3	Closed	10.7	2.3

indicating system. The drive is a 4-pole, reluctance type motor that incorporates a special 6-phase, star-connected winding shown in Figure 48. The stator coils are energized by sequential programming, producing a rotating magnetic field around the rotor assembly. This action produces rotary motion of the rollers, which rotary motion is translated into linear motion of the leadscrew. The reactor control rod is thereby raised or lowered, since it is mechanically connected and locked to the leadscrew. The SSCR drives are designed to trip whenever power to the stator is interrupted. During such a trip, the leadscrew is disengaged from the roller nuts, allowing the leadscrew and control rod to drop by gravity into the reactor core to the full "IN" position.

The position of the leadscrew within the drive is monitored by the absolute position indicator (API), which consists of a network of resistors and equally-spaced reed switches. Figures 49 and 50 show the API interconnection wiring diagrams. As the leadscrew moves vertically within the drive, a magnet attached to the drive torque-taker travels with it. Movement of the magnet past the reed switches causes those switches in the vicinity of the magnet to close. After the magnet has passed by a reed switch, the reed switch returns to its normally open condition. The arrangement of the switches is such that the closure zone for each switch overlaps approximately one-third of the closure zone of each adjacent switch, thereby providing approximately one-third clear zone with no overlap. A backup is provided by separate switches that close at 0, 25, 50, 75, and 100% positions.

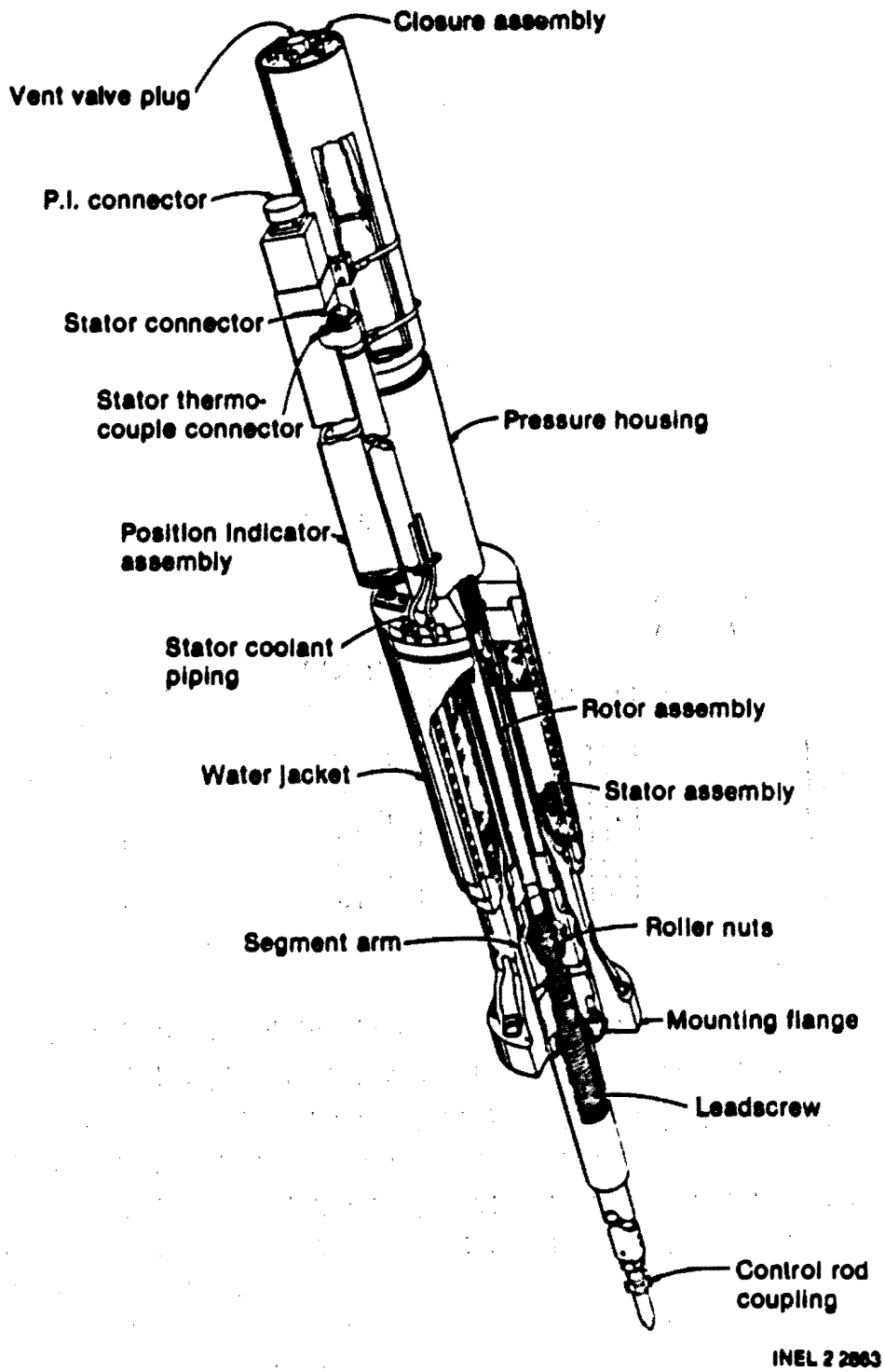

Figure 47. Typical control rod drive mechanism.

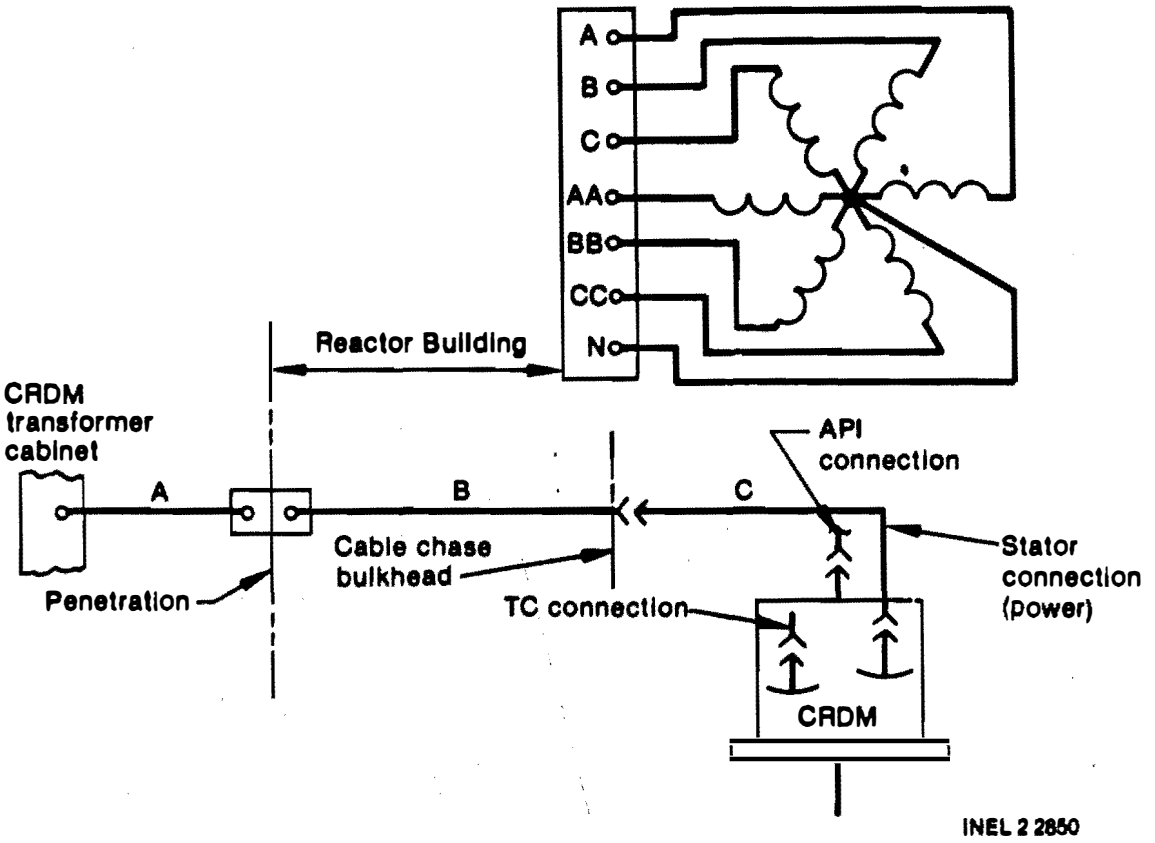

Figure 48. Control rod drive mechanism stator typical block and connection diagram.

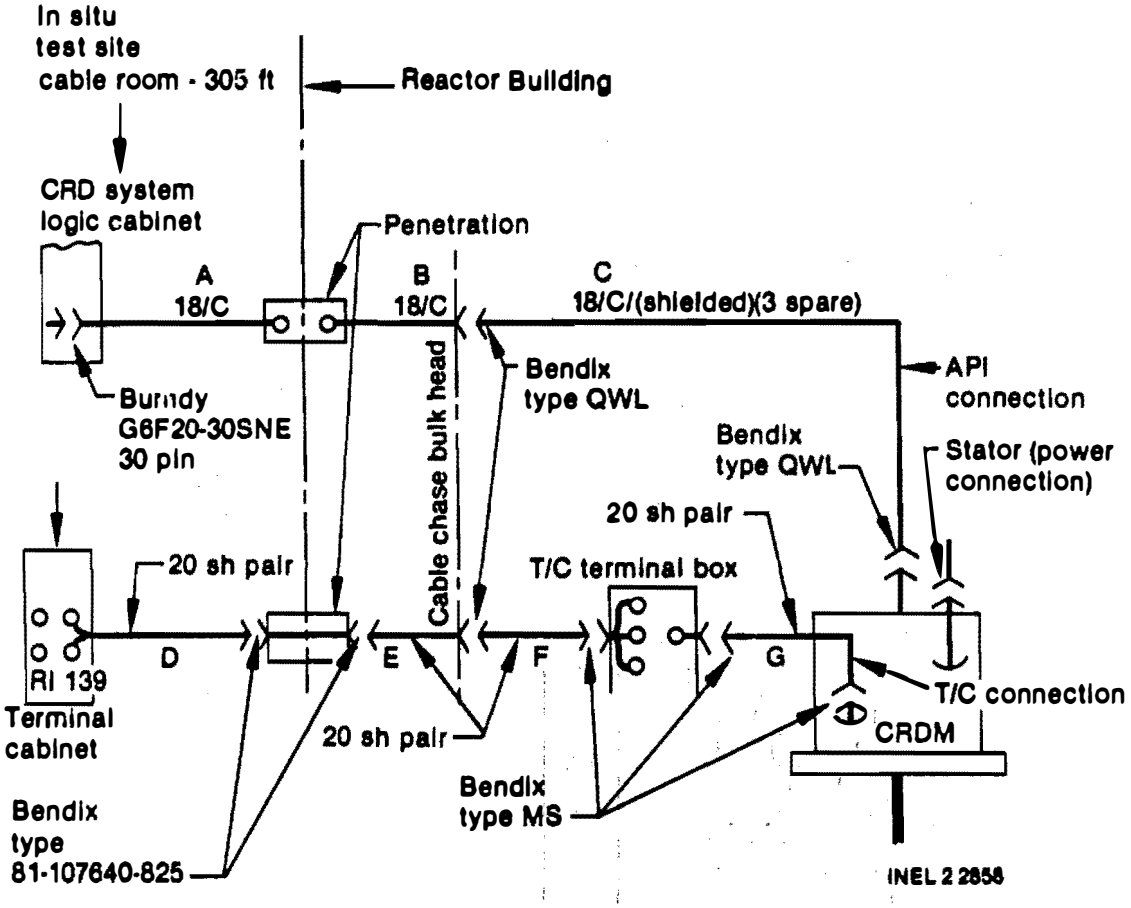

Figure 49. Block diagram of a typical CRDM absolute position indicator and stator thermocouple circuit.

CRDM-ST62 through 69 are axial power shaping rod (APSR) drive mechanism stators, and CRDM-API-62 through 69 are the corresponding rod position indicators. The mechanisms of the APSR drives and rod position indicators are almost identical to those on the SSCRs. The distinguishing difference is the presence of a builtin brake on the APSR drive. Whenever current to the stator is interrupted, the brake engages, thereby preventing rotation of the rotor assembly and disengagement of the roller nuts from the leadscrew.

CRDMs 01, 35, 50, and 62 through 69 were all subjected to static test. The APSR mechanisms (CRDM 62 through 69) were also dynamically tested. The static test data indicate that all the stator windings are apparently normal. Their dc resistances are consistent and in the range of about 7.90 ohms. Although considerably higher than the designed stator phase resistance of 5.2 to 5.82 ohms, the measured stator winding resistances are reasonable when the resistance drops at splices and connectors on the bulkhead and the service structure are considered. The inductances and capacitances are also consistent, which further supports the presumption that the CRDM stators are in satisfactory condition.

The CRDM position indicator resistor network, shown in Figure 50, consists of eight 50-ohm resistors for each mechanism. The total measured resistance of the network was in the range of 2400 ohms. See Table 4 for API dc resistance data. The resistance readings also indicate that the SSCRs 01, 35, and 50 are fully in and that the APSRs were in the 26 to 28% withdrawn position.

The thermocouples in the stators of the central control rod and 10 peripheral control rods were also tested. These thermocouples are electrically connected to Termination Box RI39 by approximately 345 ft of AWG-16 iron-constantan extension wire. The thermocouples were measured for dc resistance and temperature indication. The dc resistance data and the temperature indication are shown in Table 5. Except for Thermocouple TC2 of CRDM-22, all the thermocouples tested appear to be operational.

TABLE 4. ABSOLUTE POSITION INDICATOR DC RESISTANCE MEASUREMENT DATA (ohms)

	Pin Numbers[a]				
Control Rod	d-g	e-g	Total f-g	J-H	R-T
62	602.2	653.0	2400	Open	Open
63	603	Open	2402	Open	Open
64	604	Open	2401	Open	Open
65	602	Open	2402	Open	Open
66	602.4	Open	2402	Open	Open
67	602.4	652.3	2385	Open	Open
68	601.2	Open	2388	Open	Open
69	602.1	652.1	2401	Open	Open
01	--	--	2400	2.94	2.59
35	--	--	2400	2.1	2.50
50	--	--	2402	2.02	2.54

a. See Figure 50 for CRDM wiring diagram showing pin numbers.

The resistances are consistent and within what is expected, based on cable pulled length of 345 ft, extension wire double length resistance of 0.137 ohm/ft, and resistance data of the thermocouple assembly of 6 ± 0.5 ohms (supplied by the Diamond Power Specialty Company). Furthermore, the measurements of resistance taken from each lead to the shield verify the ratios of iron, constantan, and shield resistance. The assessed condition of the thermocouple circuits was supported by the uniformity of temperature measurements, which are commensurate with the condition at the stator location on the reactor vessel head. The location of the fault on the circuit of Thermocouple TC-2 of CRDM-22 could not be determined by means of available test instruments.

In the dynamic test of the APSRs, two rods were inserted the full 3 ft into the core; two of them were inserted to within about 7 in. of the full "IN" position; two rods moved in <7 in.; and two did not move in at all,

TABLE 5. THERMOCOUPLE LEADS RESISTANCE AND TEMPERATURE DATA

	Resistance (ohms)						Temperature (°F)	
Control Rod	I1-C1	I1-Shield	C1-Shield	I2-C2	I2-Shield	C2-Shield	TC1	TC2
30	56.66	17.50	51.85	56.59	17.33	52.14	--	--
64	53.47	16.85	49.31	52.88	16.55	48.87	--	--
22	54.67	17.29	50.69	Open	Open	Open	--	--
36	52.50	16.92	48.46	54.15	17.16	49.84	73	74
10	52.04	16.82	47.78	52.59	16.77	48.51	73	73
9	53.62	17.26	49.68	53.29	17.07	49.56	72	72
3	54.53	17.36	50.19	55.45	17.42	51.07	70	71
18	52.61	17.03	48.60	53.21	16.96	49.38	73	72
46	54.65	17.28	50.39	55.13	17.32	51.09	74	73
55	53.89	17.30	49.64	54.73	17.33	50.43	75	74
47	51.10	16.75	47.18	52.14	16.69	48.12	73	76

a. See Figure 50 for CRDM wiring diagram showing pin numbers.

although their drive rotor assemblies did latch and unlatch properly and showed minor rotational movement. APSR leadscrew final positions are shown in Table 6.

Post-Gross-Decontamination Experiment In Situ Test Results

Ten of the original 43 devices have been retested. A summary of the results is shown in Table 7. Of these retested devices, none show any obvious effect of the gross-decontamination experiment. Level Switches AH-LS-5006 and -5008 are the only devices that exhibited a mild change. AH-LS-5006 and -5008 had initially measured circuit resistances of 554 and

TABLE 6. POSITION OF APSR LEADSCREW AFTER INSERTION TEST

Control Rod Number	Final Leadscrew Position (%)	Remarks
62	5	Obstruction at 6% position
63	19	Stuck downward and upward direction
64	25	No movement even at maximum current
65	Fully in	Obstruction at 7 to 6.5% position; noisy operation between 18 to 15-1/2% and between 5 to 1% position
66	4	Noisy operation between 24 to 18% positions; obstruction from 6% to 4% positions
67	1	Obstruction at 25-1/2 to 24-1/2% positions
68	23	Stuck downward even at maximum current
69	26	No movement even at maximum current

1.81 ohms, respectively. The retest showed increased resistances of 560 and 12.2 ohms. The change on both devices took place at the devices themselves as supported by the TDR measurements shown in Figures 51 and 52 (compare with Figures 3 and 5). Since both devices are sealed units, it is surmised that the increased resistance may be due to oxide buildup on the contact surface--a phenomenon that is not likely influenced by the gross-decontamination experiment. It was also observed that the capacitive element accompanying the resistance termination of AH-LS-5006 is no longer noticeable on the TDR shown in Figure 51. This would signify that a contact suspected earlier to be wet has dried.

TABLE 7. SUMMARY OF POST-DECONTAMINATION TEST RESULTS

Equipment/Device Tag Number	Test Results	Remarks
AH-LS-5006	High contact resistance (approximately 680 ohms) termination appears purely resistive	No apparent effect of the gross decon experiment
AH-LS-5007	No change	--
AH-LS-5008	Contact resistance rose to 12.2 ohms	--
AH-EP-5037	No change	--
AH-EP-5040	No change	--
AH-EP-5037	No change	--
AH-EP-5040	No change	--
AH-V6	No change	--
NM-PS-4174	No change	--
NM-PS-4175	No change	--

CONCLUSIONS AND RECOMMENDATIONS

Fourteen electrical components and discrete devices exhibited anomalies, ranging from mild elevated switch contact resistance to a catastrophic break or discontinuity in AWG-2 and AWG-10 circuits. During the in situ testing, only one Class 1E device, NS-V100, exhibited an anomaly--a discontinunity on its CLOSED indication circuit. Many of the anomalies observed appeared on components associated with and in the vicinity of reactor coolant pump Motor RC-P-1A. Of all the observed anomalies, three types can be reasonably attributed to the accident.

The high resistance on the armature of the RC-P-1A and -2B backup oil lift pump motors and the impedance mismatch on Cable H291I exemplify the first two types of anomalies that can be attributed to the accident. Buildup of copper oxide or corrosion on the motor commutator brushes enhanced by the chemical spray during the reactor building suppression

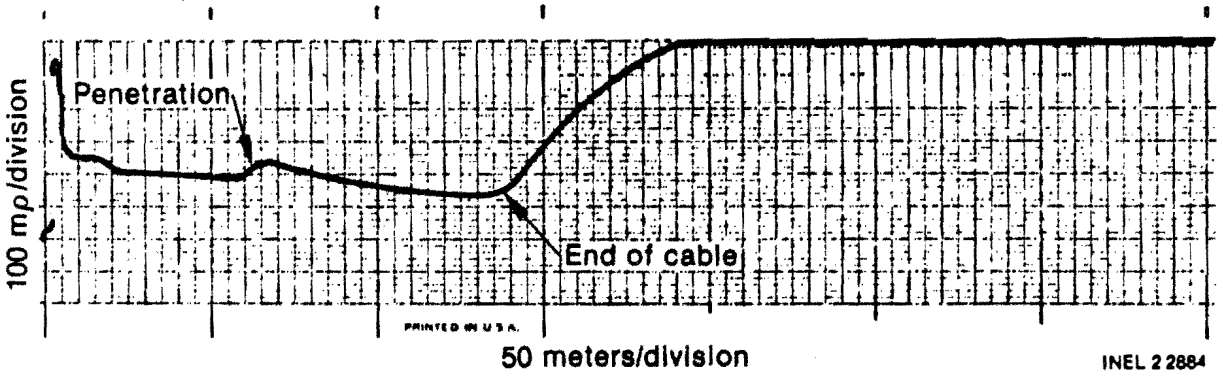

Figure 51. Post-decontamination TDR trace of AH-LS-5006.

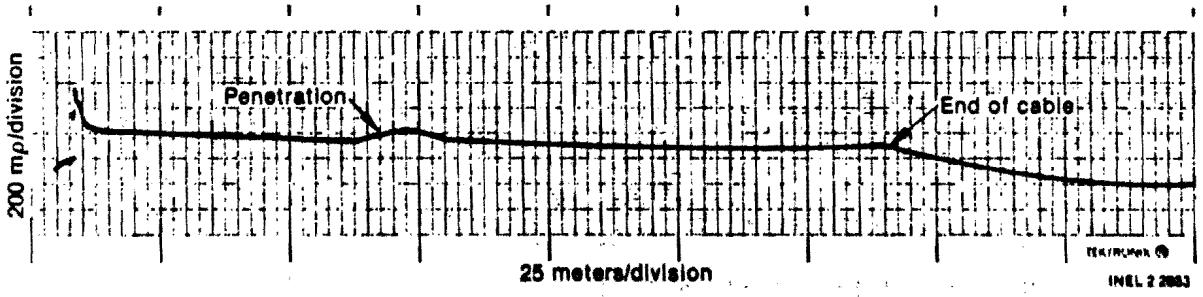

Figure 52. Post-decontamination TDR trace of AH-LS-5008.

spray event may have contributed to the high armature winding resistance. The steam and chemical spray in the reactor building during the accident may have caused wetting (impedance mismatch) of Cable H291I insulation.

The third type of anomaly that could be related to the accident is the discontinuity on two circuits in Penetration Boxes R400 and R405. These penetrations are located at the 292-ft elevation in the southwest quadrant of the reactor building. These locations were in the path of the steam originating from the reactor coolant drain tank as it rose through the open stairwell. This steam could have enhanced the corrosion process on the ring tongue terminals used in these penetration boxes, and eventually caused the connectors to break away from the terminal block.

The other anomalies are random and do not have common parameters that could relate to the affected devices. The causes and nature of the anomalies observed are still being investigated, and only conjectures can be made, based on assumptions from test data and from events that took place during and after the accident. To eliminate some of the variables used in analysis, the next step in analyzing the anomalies is to confirm the problems by physical examination where feasible. In the case of the RC-P-1A component problems, physical examination is not yet feasible. Expanded testing on additional devices in the pump area will further investigate the observed commonality in these components. Also included in the list for expanded testing are components identical to those exhibiting anomalies but associated with other reactor coolant pumps and components that have circuits using electrical Penetrations R400 and R405. A partial list of these additional components is shown in Table 8.

The in situ testing program provided some clue to the actual condition of the circuits of the equipment tested, as well as the locations of the faults. While the information gathered may not be conclusive, it will serve as good baseline data when hands-on examinations become feasible.

The best way to evaluate the condition of a component is to subject the unit to a hands-on examination; presently, this approach is seldom feasible.

Two devices have been removed from the reactor building for hands-on examination. These two devices, Pressure Switch NM-PS-1454 and the solenoid coil assembly of AH-V74, are in archival storage. Two other devices, NM-PS-4174 and the solenoid coil assembly of AH-V6, are scheduled for removal from the reactor building. The pressure switches and solenoid coil assemblies are basically identical. Off-site examinations will be performed in groups, with the grouping defined by the device type and make.

TABLE 8. ADDITIONAL EQUIPMENT FOR IN SITU TESTING

Equipment Tag Number	Equipment/Description/Type	Criteria for Selection
RC-P-2A	Reactor coolant pump motor 6900 V ac, 3-phase, 9000 hp	Identical to RC-P-1A and -2B motors
RC-P-1B backup oil lift pump motor	10 hp, 230 V dc shunt-wound motor	Identical to RC-P-1A and -2B backup oil lift pump motor
RC-P-2A backup oil lift pump motor	10 hp, 230 V dc shunt-wound motor	Identical to RC-P-1A and -2B backup oil lift pump motor
RC-P-1A backstop lube oil pump Motor 2-1A-2	1/2 hp, 480 V ac, 3-phase, 60 Hz motor	Same area as RC-P-1A
RC-P-2A backstop lube oil pump Motor 2-1A-1	1/2 hp, 480 V ac, 3-phase, 60 Hz motor	Same general area as RC-P-1A
RC-P-2A backstop lube oil pump Motor 2-2A-2	1/2 hp, 480 V ac, 3-phase, 60 Hz motor	Same general area as RC-P-1A
RC56-PS6	Barksdale pressure switch	Identical to RC56-PS1
RC56-PS11	Barksdale pressure switch	Identical to RC56-PS1
RC56-PS16	Barksdale pressure switch	Identical to RC56-PS1
RC58-FS3	M&M flow switch	Identical to RC58-FS1
RC58-FS5	M&M flow switch	Identical to RC58-FS1
RC58-FS7	M&M flow switch	Identical to RC58-FS1
RC59-FS3	M&M model flow switch	Identical to RC59-FS1

TABLE 8. (continued)

Equipment Tag Number	Equipment/Description/Type	Criteria for Selection
RC59-FS5	M&M model flow switch	Identical to RC59-FS1
RC59-FS7	M&M model flow switch	Identical to RC59-FS1
RC60-LS3	SOR pressure switch	Identical to RC60-LS1 and -LS2
RC60-LS4	SOR pressure switch	Identical to RC60-LS1 and -LS2
RC60-LS5	SOR pressure switch	Identical to RC60-LS1 and -LS2
RC60-LS6	SOR pressure switch	Identical to RC60-LS1 and -LS2
RC60-LS7	SOR pressure switch	Identical to RC60-LS1 and -LS2
RC60-LS8	SOR pressure switch	Identical to RC60-LS1 and -LS2
RC67-VS2	Robertshaw vibration switch	Identical to RC67-VS1